Survey of Blunt Body Dynamic Stability in Supersonic Flow

Cole D. Kazemba[1,2]
Georgia Institute of Technology, Atlanta, GA 30332-0150
Science and Technology Corp., Moffett Field, CA 94035

Robert D. Braun[3]
Georgia Institute of Technology, Atlanta, GA 30332-0150

Ian G. Clark[4]
NASA Jet Propulsion Laboratory, Pasadena, CA 91109

and

Mark Schoenenberger[5]
NASA Langley Research Center, Hampton, VA 23681

This survey presents a comprehensive investigation of blunt body dynamic stability. An examination of the experimental, analytical, and computational methods for predicting dynamic stability characteristics, along with the deficiencies accompanying each method is presented. The observed influence of vehicle and environmental parameters on the resulting dynamic response is discussed. Additionally, the proposed physical mechanisms that may govern this complex phenomenon are introduced. There exists a vast amount of literature and test data that is continually growing with each mission. Compiling the observations of dynamic behavior acquired from various test geometries, environments, and techniques, as well as the proposed explanations to the observed trends, sheds light on the validity of the proposed physical mechanisms. This in turn guides future efforts to improve the experimental and computational prediction techniques and further the fundamental understanding of blunt body dynamic stability.

Nomenclature

A	=	Aerodynamic reference area, m^2
C_D	=	Drag coefficient
C_L	=	Lift coefficient
C_{L_α}	=	Lift-curve slope
C_m	=	Pitching moment coefficient
C_{m_α}	=	Pitching moment slope
C_{m_q}	=	Pitch damping coefficient
$C_{m_q} + C_{m_{\dot{\alpha}}}$	=	Pitch damping sum
CG	=	Center of gravity
D	=	Reference diameter, m
DOF	=	Degrees of freedom
f	=	Oscillation frequency, Hz
g	=	Acceleration due to gravity, m/s^2
h	=	Altitude, m

[1] Graduate Research Assistant, Guggenheim School of Aerospace Engineering. Student Member AIAA.
[2] Research Scientist/Engineer, NASA Ames Research Center
[3] Professor, Daniel Guggenheim School of Aerospace Engineering. Fellow AIAA.
[4] Aerospace Engineer, Entry, Decent, and Landing Systems and Advanced Technologies Group, Member AIAA
[5] Aerospace Engineer, Exploration Systems Engineering Branch, Member AIAA

I	=	Moment of inertia, kg-m^2
k	=	Reduced frequency parameter
l	=	Characteristic length, m
m	=	Mass, kg
R	=	Radius from center of planet, m
Sr, St	=	Strouhal number
t	=	Time, s
V	=	Velocity, m/s

Greek

α	=	Angle of attack, rad
γ	=	Flight path angle, rad
θ	=	Pitch angle, rad
ξ	=	Dynamic stability parameter
ρ	=	Atmospheric density, kg/m^3
ω	=	Angular velocity, rad/s

Subscripts

∞	=	Freestream condition

I. Introduction

IN the continued exploration of our Solar System, science objectives often require for the landing of a payload on the surface of a body with a sensible atmosphere. Examples of missions falling into this category are those visiting Mars, Venus, Titan, or any mission that must return crew or science payload to Earth. Due to heating constraints, these vehicles are generally blunt in shape [1]. Unfortunately, these blunt shapes are generally dynamically unstable once they reach the low to mid supersonic portions of their trajectory. Thus, their oscillation amplitudes will diverge until equilibrium is attained and a limit cycle amplitude is reached.

Initial investigations into the phenomenon of dynamic stability as applied to blunt bodies began in the 1950's as the development of ballistic missile and space exploration technologies gained momentum. At that point, dynamic instability was an issue familiar to the aerospace community due to its prevalence in aircraft dynamics. However, due the drastically different operational environments and geometries of entry vehicles, engineers lacked intuitive insight into the problem at the early stages. The analytical work of Allen [1] and Tobak [2] combined with extensive experimental investigations by Bird [3], Fletcher [4],[5], Short and Sommer [6] and others [7]-[12] helped to develop this intuition. These studies also highlighted the unpredictable nature of blunt body dynamic stability, its sensitivity to geometric and environmental variables, and the difficulties associated with determining the stability parameters analytically, numerically, or experimentally. Even with significant experimental effort and computational development since this early era of research, the same uncertainties regarding the driving physical mechanisms behind dynamic stability and difficulties in predicting dynamic performance persist today.

A. Vehicle Design and Mission Implications

The dynamic response of a body is strongly coupled to both vehicle design criteria and mission objectives. Thus, accurately quantifying and effectively minimizing the expected oscillation amplitude along the entry trajectory has significant implications on the entire system.

1. Vehicle Design Considerations

The most significant vehicle design aspects that affect dynamic stability are the overall geometry and mass properties of the vehicle. Forebody shape, aftbody shape, shoulder radius, center of gravity location, and other parameters all influence the dynamic stability characteristics. If a vehicle employs a reaction control system to counteract the dynamic oscillations, this system must be sized and designed to meet the requirements given from an estimated dynamic response. In addition, the heating environment experienced by the body will be altered by the angle of attack history; therefore, the sizing of the thermal protection system of a vehicle must take into account the oscillation amplitudes that are to be experienced during entry.

2. Mission Design Considerations

In addition to impacting the design of systems and subsystems of the vehicle itself, dynamic stability issues have a critical role in many aspects of the mission design. For any vehicle employing a parachute, it is critical that the oscillation amplitude at the time of parachute deployment be less than approximately 10^o to ensure proper inflation [13]. Entry trajectory design is a significant driver of a vehicle's dynamic response through a dependence on Mach number, Reynolds number, Strouhal number, and dynamic pressure. Additionally, trajectory dispersions, the size of the landing footprint, atmospheric science performed during entry, and on board communication capabilities may be sensitive to angle of attack oscillations.

B. Governing Equations of Motion

It is informative to examine the equations of motion that describe the dynamic oscillation of a vehicle such that the subsequent discussions on the influence of various parameters in the system are grounded in the context of the governing physics. Thorough derivations of the differential equations governing the pitching motion of an entry vehicle as a function of time, typically starting from the planar equations of motion, can be found in the literature [1],[2],[13]-[15]. Figure 1 describes the coordinate system of the planar formulation of the problem. A brief derivation presented here also begins with four planar equations of motion for an entry vehicle that describe rates of change of the altitude, velocity, flight path angle, and pitch angle with respect to time:

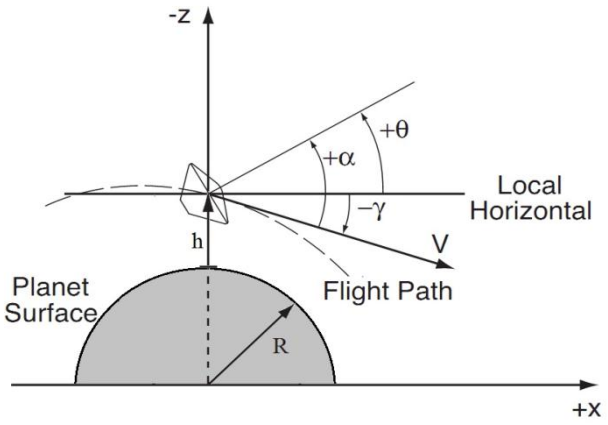

Figure 1. Reference Coordinate System [15]

$$\frac{dh}{dt} = \dot{h} = V \sin\gamma \tag{1}$$

$$\frac{dV}{dt} = \dot{V} = \frac{-\rho V^2}{2}\frac{C_D A}{m} - g\sin\gamma \tag{2}$$

$$\frac{d\gamma}{dt} = \dot{\gamma} = \frac{\rho V A C_L}{2m} - \left(\frac{g}{V} - \frac{V}{R}\right)\cos\gamma \tag{3}$$

$$\frac{d^2\theta}{dt^2} = \ddot{\theta} = \frac{\rho V^2 A D}{2I}\left(C_{m_q}\frac{\dot{\theta}D}{2V} + C_{m_{\dot{\alpha}}}\frac{\dot{\alpha}D}{2V} + C_{m_q}\alpha\right) \tag{4}$$

Inherent to this description of the motion are several simplifying assumptions:

- Motions are restricted to a plane
- Aerodynamic derivatives are independent of Mach number and vary linearly with α
- Small L/D
- Small angle of attack ($\alpha < 30^o$) [15]
- Constant acceleration due to gravity
- Spherical, non-rotating planet
- Constant mass vehicle
- No contribution of atmospheric winds

If we apply one further assumption to Eqs. (1-3), namely that the contributions of the gravitational and centrifugal forces are negligible, the resulting differential description of the angle of attack can be obtained:

$$\ddot{\alpha} + \left(\frac{\rho V A}{2m}\right)^2 C_D C_{L_\alpha}\alpha + \left(\frac{\rho V A}{2m}\right)C_{L_\alpha}\dot{\alpha} = \frac{\rho V^2 A D}{2I}\left(C_{m_q}\frac{\dot{\theta}D}{2V} + C_{m_{\dot{\alpha}}}\frac{\dot{\alpha}D}{2V} + C_{m_q}\alpha\right) \tag{5}$$

Often, it is further assumed that the rate of change of angle of attack is much greater than that of the flight path angle and that terms which manifest as small modifications of the frequency of oscillation can be neglected [15]. What remains is a closed form differential equation describing the time evolution of angle of attack for an entry vehicle:

$$\ddot{\alpha} - \frac{\rho V A}{2m}\left[-C_{L_\alpha} + \frac{mD^2}{2I}\left(C_{m_q} + C_{m_{\dot{\alpha}}}\right)\right]\dot{\alpha} - \frac{\rho V^2 A D}{2I} C_{m_\alpha}\alpha = 0 \tag{6}$$

3. Analytical Applications of the Equation of Motion

In the literature, Eqs. (5) and (6) above have been manipulated to obtain analytical descriptions of key parameters or special cases which are useful in developing intuition and gaining insight into the expected dynamic response. By using an exponential atmosphere and other assumptions, Allen [1] was able to find an analytical expression for the velocity as function of altitude. By implementing this into the relations above, he then introduced a dynamic stability criterion:

$$\xi = C_D - C_{L_\alpha} + \frac{D^2 m}{I}\left(C_{m_q} + C_{m_{\dot{\alpha}}}\right) \tag{7}$$

where $\xi < 0$ would indicate a dynamically stable configuration. Fig. 2 displays this parameter as a function of cone angle and location of the center of gravity for conical missile shapes. It can be seen that at the high cone angles typically used for entry vehicles due to heating concerns, the parameter becomes less negative which indicates the body is less dynamically stable.

This criterion is similar to using a negative lift curve slope as an indicator that a vehicle is statically stable. While this parameter is useful for understanding the trends of dynamic stability, the numerous assumptions behind its derivation require that it be used with caution, as a negative ξ does not guarantee a dynamically stable vehicle. Often, in the literature and throughout this report, the pitch damping sum $\left(C_{m_q} + C_{m_{\dot{\alpha}}}\right)$ from the dynamic stability parameter is used independently as a measure of dynamic stability, with negative values indicating positive (favorable) damping. This term is effectively a measure of the damping experienced during small oscillation perturbations about a mean angle of attack [16].

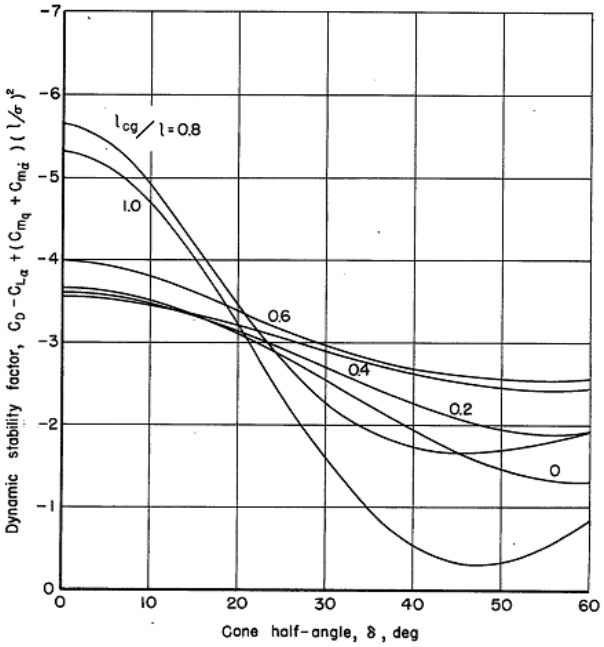

Figure 2. Dynamic stability parameter for various conical missile shapes [1]

Using the same closed form solution for the velocity as in [1], multiple studies formulated expressions for bounding the maximum oscillation amplitude and frequency [1],[2],[14],[17]. More recently, Schoenenberger et al [15] solved Eq. (6) with the Euler-Cauchy equation and used this solution to study the simplified oscillatory behavior of a body in which additional assumptions of a body in free flight ground testing apply.

These analytical formulations are useful in understanding the fundamentals of the dynamic stability phenomenon. However, the numerous assumptions made do not accurately capture the complex nature of the flow field around a blunt body and limit their use as design and analysis tools.

C. Structure of a Blunt Body Wake

There is consensus within the field that unsteady pressure forces on the aftbody are the primary source of dynamic instability. This problem was not as evident in the early investigations of the dynamic stability of ballistic missile shapes because of the relatively well behaved convergent flow behind the long, slender bodies being studied.

As the focus changed from ballistic missiles to blunt capsule shapes with the rise of the space race, it became clear that an understanding of the aftbody flow structure was critical to understanding the dynamic stability phenomenon.

In supersonic flow about a blunt body, a bow shockwave leads the nose of the vehicle. Flow downstream of the bow shock stagnates on and accelerates around the forebody. The large turning angle off the shoulder induces the formation of expansion waves and separation of the flow. This creates a low-pressure region behind the body characterized by an unsteady recirculation region in the near wake. Further downstream, the wake flow converges, stagnates and forms a trailing recompression shock that heats the fluid. Fig. 3 graphically depicts these flow features. The core of the wake will be viscous and often partially subsonic while the outer wake is typically inviscid and supersonic. Even in steady flight with zero angle of attack, these factors combine to result in a flow with a time-varying pressure field is a function of axial and radial position relative to the forebody.

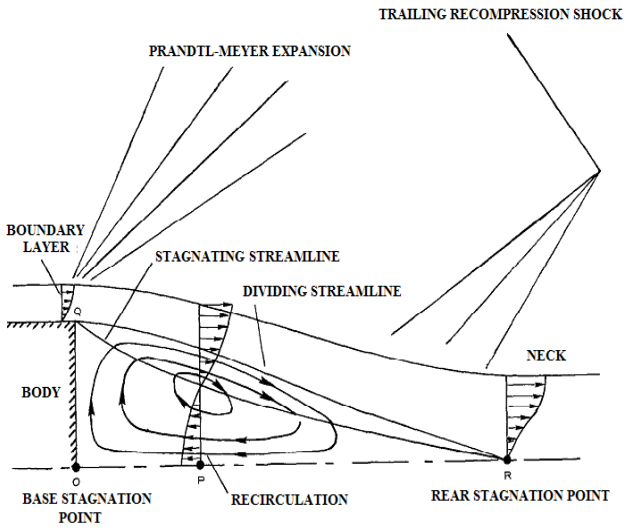

Figure 3. Flow structure behind a blunt body [18]

When pitch oscillations are added to this scenario, the position of the wake features "lag" behind the motion of the forebody due to the finite convection velocity in the flow. This creates a hysteresis effect on the pitching moment and aft body pressure field, adding further complexity to the wake structure [19]. At present, no experimental or computational methods have accurately and generally captured the time-varying, dynamic wake structure of a blunt body undergoing pitch oscillations. Large uncertainties in the behavior of the aft body wake prevent a clear understanding of dynamic stability phenomena.

II. Experimental Techniques for Characterizing Damping

Experimental methods for determining the dynamic stability characteristics of a blunt body have roots in methods developed for aircraft. Captive techniques involve the use of a classic wind tunnel setup with variations in the sting functionality such that the body can undergo pitch oscillations. In addition to these more traditional methods, sub scale free flight techniques have also been developed which can yield the damping behavior of a body without the intrusive effects of a sting tarnishing the results. Existing methods have significant deficiencies with regard to either accuracy or validity of the damping characteristics. Thus, to minimize uncertainty, two or more of these techniques are often used when building an aerodynamic database of a new vehicle.

A. Forced Oscillation Testing

Dynamic wind tunnel testing with a forced oscillation setup generally uses an axial sting that measures forces and moments, as well as the rates of change of these parameters with respect to changing pitch angle or angle of attack. In order to capture the dynamic behavior, a motor attached to the sting imparts a one-degree-of-freedom oscillatory motion to the vehicle at a wide range of frequencies and mode shapes. Sinusoidal motion is typically used [20]. The vehicle is inclined at a wide range of angles of attack and at each condition undergoes a series of small amplitude pitch oscillations. The damping response of the vehicle is measured as a function of pitch amplitude, angle of attack, and Mach number. Advantages

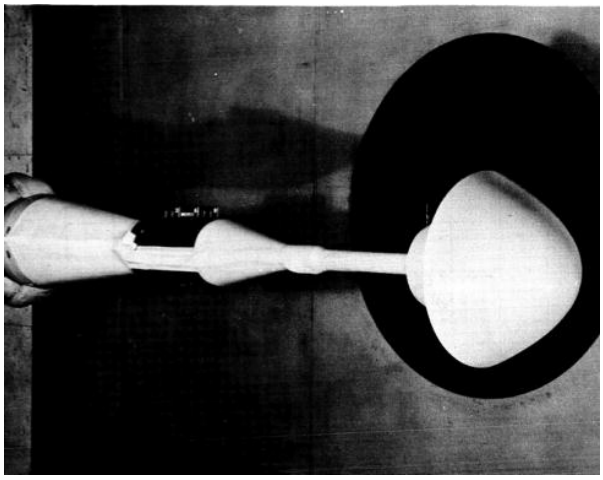

Figure 4. Forced oscillation setup [22]

of this technique are its direct measurement of the dynamic aerodynamic coefficients [15],[20], controllability and repeatability [14], and its ability to match a wide range of reduced frequency parameters (also known as Strouhal numbers) [13]. Additionally, mass scaling is not generally required to obtain representative full scale behavior in the sub scale environment [20]. Drawbacks of forced oscillation tests are the sting effects on the damping and the inability to observe limit cycle behavior [15]. Also, due to the nature of the the test setup itself, only the average damping over a pitch cycle can be obtained [21] and the accuracy to which it can be obtained is reduced as the measurement techniques are reliant on three independent strain gauge force measurements [20].

B. Free Oscillation Testing

Free oscillation uses a transverse rod positioned through the center of rotation of the vehicle. This rod is set in low friction bearings that allow the model to pitch freely in response to the oncoming freestream flow. Following an initial oscillatory perturbation, the vehicle's natural dynamic damping response is measured. By observing the time history of the oscillatory growth or decay, the dynamic aerodynamic coefficients can be determined with parameter identification techniques. This technique was matured during the Apollo program and is still in use today. It allows for explicit determination of the reduced frequency inherent to the vehicle (as opposed to sweeping through various possibilities as in forced oscillation technique) [20], is simple in its implementation, and requires only one measurement (oscillation amplitude as a function of time) [13]. Similar to the forced oscillation setup, free oscillation testing yields an average value of the damping over one oscillation cycle and suffers from the effects of having a sting present to modify the wake flow. Also, it has additional scaling requirements in that the center of gravity of the vehicle must be coincident with the center of rotation and the pitch moment of inertia must be scaled properly from the expected full scale vehicle for representative behavior to be obtained [21]. Finally, damping due to bearing friction must be accurately quantified so that it can be separated from the aerodynamic damping of the vehicle.

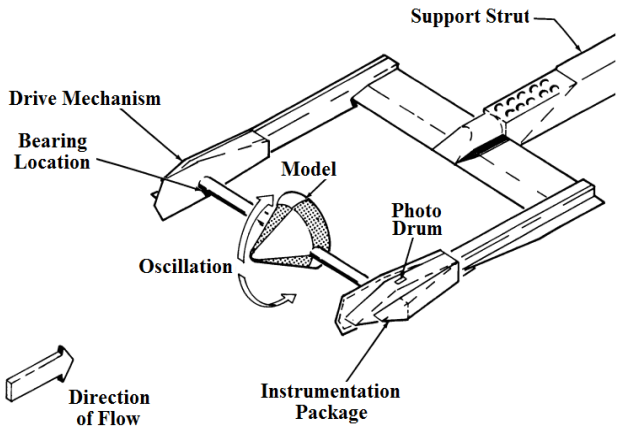

Figure 5. Free oscillation setup [22]

C. Free Flight Wind Tunnel Testing

There is significant desire to obtain the damping behavior of a vehicle in a representative free flight environment without the limitations and interferences introduced by the captive methods. One such way to obtain those conditions is free flight wind tunnel testing. This method consists of a model that is either shot upstream into the flow with a pneumatic or ballistic gun or simply cut free and allowed to fall from a suspending wire. The goal of these approaches is to observe the vehicle in the test section of the wind tunnel with schlieren photography and high speed video to capture the wake structure and pitching behavior. This method allows for well-controlled initial and environmental conditions relative to ballistic range tests [13],[14] as well as characterization of the sting-free wake geometry at near constant speed with schlieren imaging [22]. Finally, the greatest advantage of this method is the true, 6 DOF dynamics that are obtained by a properly scaled vehicle as opposed to the restricted pitching motions of the free and forced oscillation testing.

This method is not without disadvantages, however. First, proper dynamic scaling of mass, moment of inertia, and Reynolds number must be taken into consideration to obtain behavior representative of the full scale vehicle. Also, given the limited size of the observable test section within a wind tunnel, the number of oscillation cycles which are observed is often limited. The number of cycles can be modified with proper design and scaling of the model, however, these parameters are limited by the camera and launching systems, as well as the ability to match the required similitude requirements. In addition, obtaining the damping coefficients relies on estimating the position and oscillation history as a function of time, as opposed to a direct measurement.

D. Ballistic Range Testing

Similar to the free flight wind tunnel methods, ballistic range testing offers free flight dynamic behavior without the constraints imposed by captive methods. A geometrically and mass scaled model is shot from a gun down a range past stations where the position, velocity, and orientation are recorded along with the current time step. Fig. 6 depicts the two simultaneous schlieren imaging stations at the Eglin AFB Aeroballistic Research Facility [15]. From these discrete measurements, the trajectory and oscillation history can be estimated. Given the nonlinear nature and Mach number dependence of the dynamic aerodynamic coefficients, there are a range of functional forms that can fit the observed data points. Thus, the shots are repeated at a variety of initial angles of attack and Mach numbers across the operational space to improve the determination of the functional form of the aerodynamic coefficients [15].

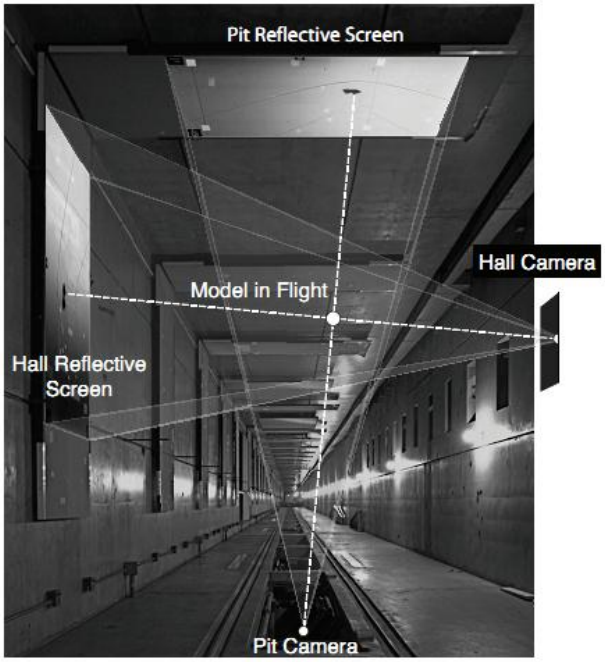

Figure 6. Schlieren imaging station at Eglin AFB ARB [15]

Ballistic range testing is generally chosen over free flight wind tunnel testing because it offers more pitch cycle observations and thus less uncertainty when reducing the data. In addition to the advantage of true dynamic behavior, ballistic range testing also offers the ability to observe the oscillation behavior of a decelerating vehicle. This is important for blunt entry vehicles, which have often been observed to exhibit instabilities in the presence of waning dynamic pressure [23]. Although ballistic range tests best recreate the dynamics of the true full scale vehicle, the indirect measurement of the dynamic aerodynamic characteristics and limited control over the initial conditions often result in large uncertainties. Additionally, constructing models to match the scaling conditions and withstand the extreme accelerations upon launch introduces design challenges and limitations.

E. Sting Effects on Dynamic Testing

One significant drawback of both forced and free oscillation testing techniques is the influence of the sting on the resulting aerodynamic parameters. The interference due to the sting is induced through both a structural coupling with the oscillation of the sting structure and an aerodynamic coupling via the sting's alteration of the wake geometry and aerodynamic loading of the vehicle [24]. This influence has been noted throughout the literature and much effort has been put towards circumventing sting effects. Modifications to sting geometry, empirical methods to extrapolate sting size to zero, and analytical formulations have been attempted with the goal of quantifying and minimizing the effect of a sting during a dynamic test. Although minimal success has been obtained from these investigations, several informative observations have been made which shed light on the impact of a sting and thus provide insight into the dynamic stability phenomenon.

1. Critical Sting Size

Many of the investigations focused on finding the optimal sting length and diameter such that sting effects would be minimized. Wehrend [12] conducted much of this work and typical investigations of the effect of sting length and diameter are shown in Fig. 7. His results indicate a relative insensitivity to sting lengths beyond twice the maxiumum diameter of the vehicle. Uselton and Cryon [25] found similar critical sting lengths for slender cones by using pressure measurements at various locations on the bodies.. During the investigation for the Viking configuration [26], sting length was found to have a negligable effect on wake geometry and damping characteristics except for low Reynolds number flow ($0.25\text{-}0.75 \times 10^6$) at M=1.76 and angles of attack near zero. Unfortunately, the regime where sting effects were shown to be prominant is also the regime in which instabilities are typically greatest. This is likely not a coincidence and reiterates the difficulties which face researchers trying to use experimental methods to characterize the dynamic response of blunt bodies.

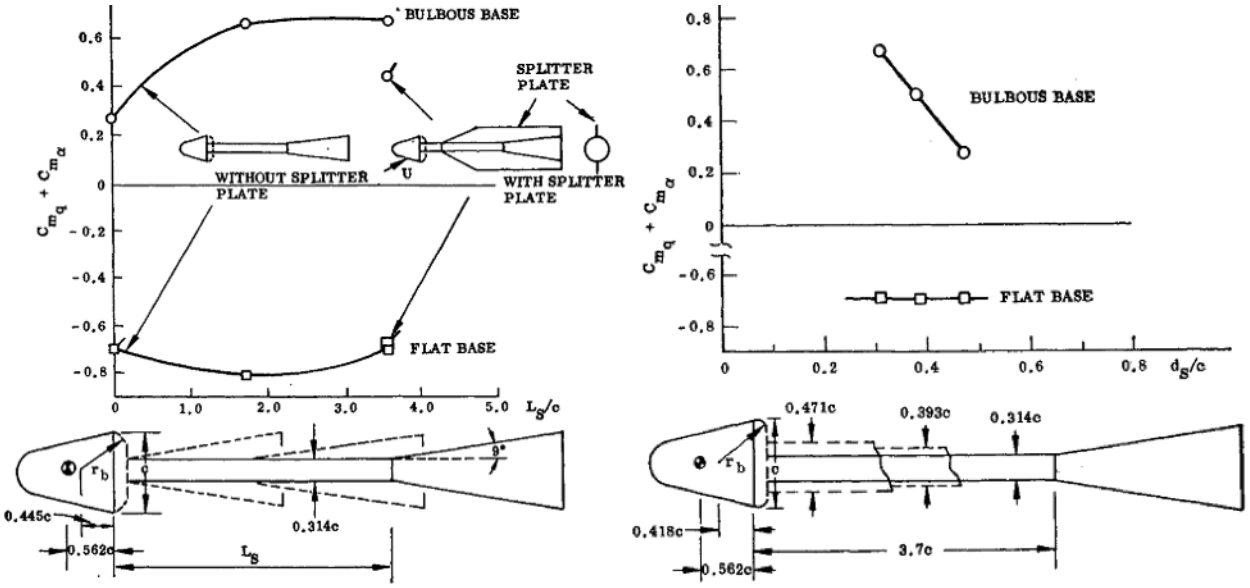

Figure 7. Effect of sting length (left) and diameter (right) at M=0.65 [24], adapted from [12]

Investigations into the ciritcal sting diameter for which sting effects are negligable have shown some contradictory results. Wehrend [12] found insensivity for Mach numbers of 1.60 and 1.00 for both flat based and spherically ("bulbous") based models. However, at M=0.65 he found the damping of the spherically based model increased with increasing sting diameter

2. Axial and Transverse Sting Effects

With knowledge that the near wake and its effects on the aftbody have a significant influence on the dynamic stability characteristics of a vehicle, efforts to reposition the forced oscillation sting to eliminate its contributions to the aftbody pressure field (and thus damping) have been. Dayman et al [14] suggest use of a transverse sting (crossing through the center of rotation of the vehicle) for Mach numbers greater than 3 or when studying damping at high angles of oscillation because the wake interference is "restricted to the sides of the aft portion of the model, where aerodynamic forces in the pitch plane are probably minor" for the class of models which were investigated. However, they cite earlier work by Dayman [27] that found significant alteration of the wake geometry for transverse supports as small as 2.5% of the model diameter and caution that dynamic response with a transverse sting is not to be assumed to be perfectly representative of free flight behavior. Reding and Ericsson [24],[28] compared the pitch damping of slender, bulbous-based, blunted cones with transverse and axial sting arrangements and found vast differences in the resulting dynamic response at Mach numbers between 1 and 2 (Fig. 8). Again, the largest discrepancies arise in the regime where dynamic stability issues are most critical. Their studies suggested that the transverse sting arrangement introduced an undamping effect on the vehicle while the axial sting improved damping. They point to the loads induced by the presence of a sting and their convective time lag in the near wake as the source for the interference for both sting configurations (Fig. 9) [24],[28]. Accepting that it will be

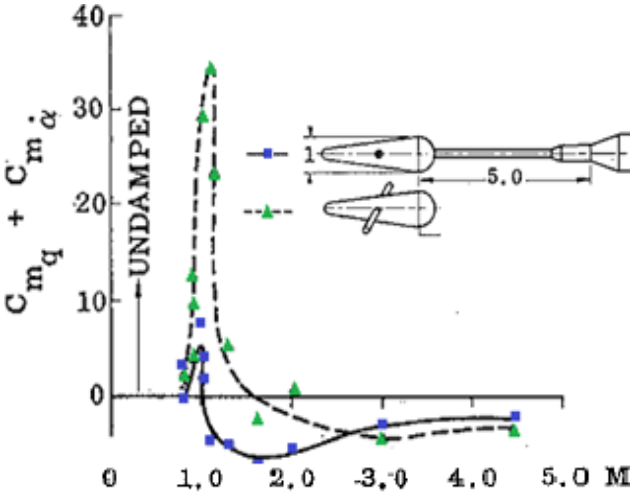

Figure 8. Pitch damping with axial and transverse sting arrangements [24],[28]

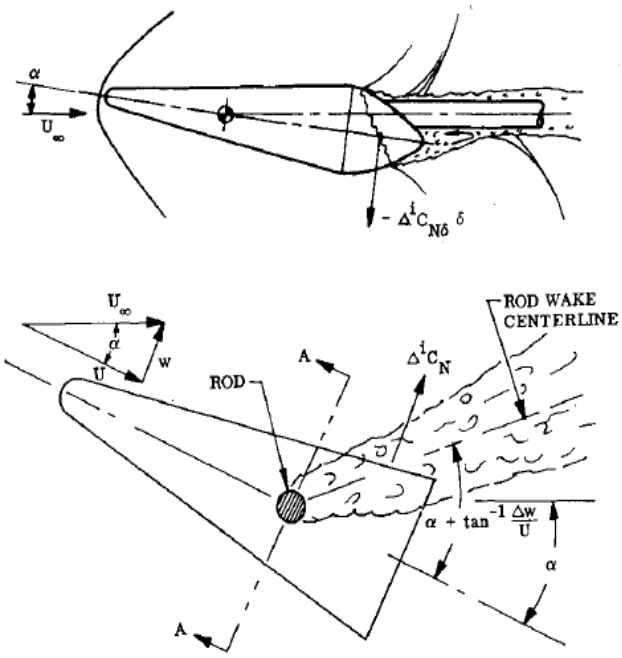

Figure 9. Axial and transverse sting wake interference and induced loads [24],[28]

exceedingly difficult to eliminate the influence of either sting setup, they propose a "quasi-steady" technique to correct for the influence of the stings. This method combines interference loads and communication speeds within the wake (both determined from through measurements taken during static experiments) to ascertain the approximate induced normal loads. This technique assumes a small sting (i.e. neglects effects of the alteration of the wake geometry due to its presence). Using this technique, they site experimental extrapolation to zero sting size as a possible way to totally account for the effects, although getting a sufficiently small sting to ensure a confident extrapolation is difficult without sacrificing the required stiffness.

During recent aerodynamic characterization of the Orion Crew Module by Owens et al [20], a trade study on the sting angle for a forced oscillation test was conducted to determine if the sting geometry had a significant impact on the damping results. The damping was measured with the sting in an axial arrangement (0^o) and with an entry angle of 27.5^o. The results for the subsonic and transonic Mach numbers are shown in Fig. 10. It can be seen that the sting setup has a great influence on the resulting dynamic aerodynamic characterstics of the vehicle. As a result of this conclusion, a new transverse sting setup was implemented into the Langley Transonic Dynamics Tunnel (TDT), capable of doing forced oscillation, free oscillation, and static testing without changing the test setup (Fig. 11). Like Reding and Ericsson [24],[28], it was thought that the transverse sting arrangment would only affect the flow on the aftbody and be less intrusive on the near wake (and therefore dynamic response). The primary intention of the transverse setup was to reduce the angle of attack dependence of the sting effects.

3. Additional Sting Issues

In addition to issues regarding the sting diameter, length, and physical placement on the test model, further issues regarding the presence of the sting were also observed during testing. The shape of the axial sting in a forced oscillation test was examined and a cylindrical sting was found to impart a damping effect [24],[29]. In one study [24] it was found that using a flared sting produced an undamped effect. However, in Ref. [25], the authors found the effect of a similar arrangement employing a splitter plate on the sting to be inconclusive. Finally, it was observed that the sting effects, like the dynamic stability in general, are highly dependent on geometrical and envionmental parameters in the test setup [24]. It is clear that poor understanding of the physical mechanisms which govern dynamic stability prevent a clear understanding of sting effects in captive testing techniques.

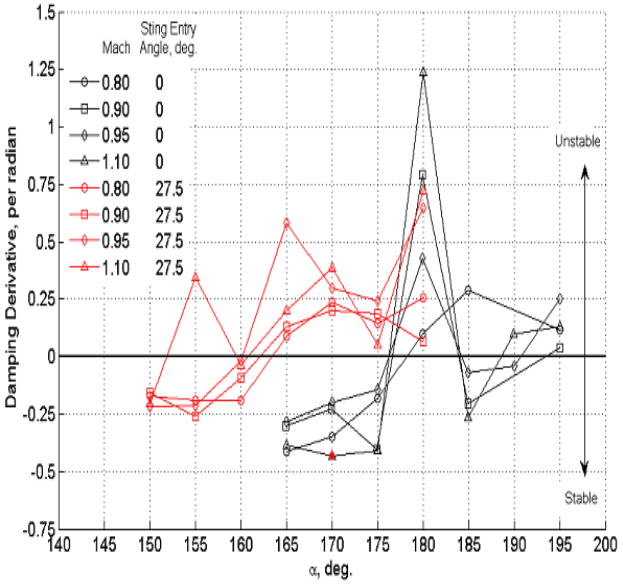

Figure 10. Orion crew module damping with sting entry angles of 0^o and 27.5^o [20]

F. Overall Deficiencies in Testing Capabilities

In reviewing the candidate methods used for obtaining dynamic aerodynamic performance of vehicles, it is clear that there is no one method which

can provide results without introducing significant uncertainties inherent to either the test setup or data reduction. For the captive methods of forced and free oscillation, sting effects are the most considerable disadvantage as they are highly dependent on the test conditions, difficult to quantify, and not generally understood. Additionally, the captive methods only provide single-axis behavior and cannot capture true rotational dynamics. The free flight methods avoid the sting effects and can recreate the true dynamic performance of the full-scale vehicle to a high degree. However, their greatest shortcomings are in the uncertainty of post processing of the discrete data points to estimate the trajectory and the difficulties in matching scaling parameters and desired initial conditions. Key traits of each of these test methods are summarized in Table 1.

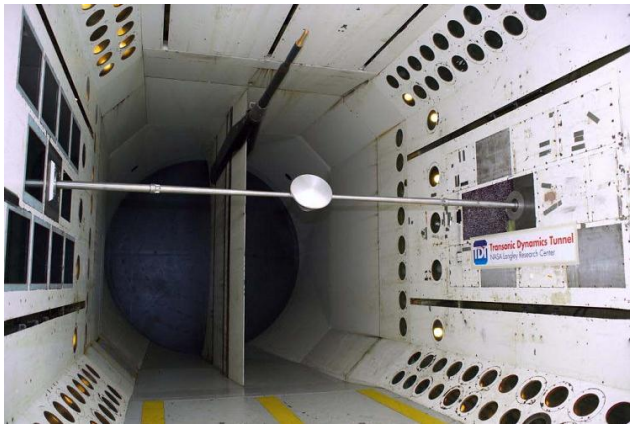

Figure 11. Transverse sting arrangement in the NASA Langley Transonic Dynamics Tunnel [19]

Table 1. Traits of dynamic testing methods

	Observed Motion	Sting Effects	Measurement	Scaling Requirements
Forced Oscillation	1-DOF Forced Sinusoidal Pitching	Axial or Transverse	Direct: Three independent forces	None
Free Oscillation	1-DOF Free Pitching Motion	Transverse	Indirect: Continuous trajectory reconstruction	Must have center of rotation and CG coincident, Sr
Free Flight Wind Tunnel	True 6-DOF with few cycles	None	Indirect: Discrete point trajectory reconstruction	Must match Re, M, I, m, Sr simultaneously
Ballistic Range	True 6-DOF with multiple cycles	None	Indirect: Discrete point trajectory reconstruction	Must match Re, M, I, m, Sr simultaneously

Given the deficiencies of each method, aerodynamicists typically employ several of these techniques in an effort to combine the results and reduce uncertainties. This can be demanding on the resources of a project. In future research on the physical mechansims which drive dynamic stability phenomena, attention must be paid to how these mechanisms will influence testing such that improvements in test methodology may be made and the error bars on the dynamic aerodynamic performance reduced.

III. Numerical Prediction Methods

A. Semi-Empirical Impact Methods

There is great motivation for the development of adequate prediction methods using numerical techniques. To obtain the aerodynamic characteristics, accurate prediction of the time varying pressure field acting on the body is required. For the static case at hypersonic Mach numbers, Newtownian impact methods are used to approximate the lift, drag, and moment coefficients as well as their derivatives. In order to apply impact techniques to the dynamic case, modified methods have been developed. One of these methods, known as embedded Newtonian, "accounts for the reduced dynamic pressure and lower flow velocity in the embedded flow downstream of the strong bow shock" [30]. This semi-emprical inviscid technique was first introduced and developed by Seiff [31]-[33] and extended to the unsteady case by Ericsson [34] for infinite Mach numbers. Further development by Ericsson [35] generalized this theory to finite Mach numbers, with good agreement for sharp slender cones down to M=3 (see Fig. 12). In this method, as Mach number increases, the approximation approaches the experimental results. Ericsson notes, however, that the effect of cone angle in these results is inconsistent. Although he applies this method to sharp blunted cones, the method is not developed for application to the high drag, blunt bodies generally used in planetary entry missions.

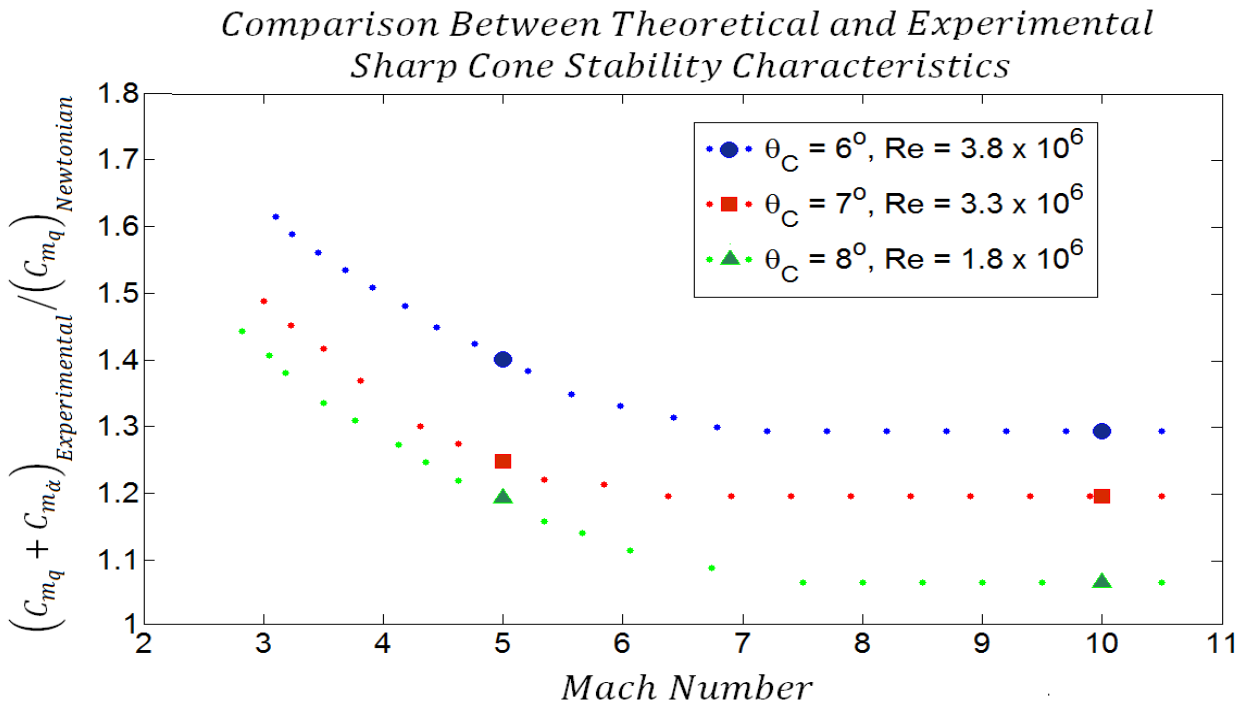

Figure 12. Comparison between theoretical and experimental sharp cone stability characteristics [35]

The method of Ericsson [35] was extended by Tong and Hui [36] with the addition of the Busemann correction for the centrifugal forces within the shock layer. Their work improved results for blunt bodies relative to the underpredicting method of [35], although demonstration of this improvement was limited to low hypersonic Mach numbers. The results of [36] were examined by East and Hutt [30] for sharp and blunt 10^{o} cones as well as a slender, flared blunt cylinder, demonstrating that with proper empirical Mach number relations, the centrifugal force correction of the Busemann theory would overpredict damping and suggesting that the theory developed by [36] be applied only in the cases where $M \to \infty$ and $\gamma \to 1$. Predictions from both methods are demonstrated for relatively sharp bodies with results that differ substantially from the available experimental data under certain conditions due to the complexities in the flow environment [30].

B. Computational Fluid Dynamics (CFD)

Employing state-of-the-art CFD tools to predict dynamic stability has been attempted in recent years in an effort to build on the semi-empirical methods. Murman [37],[38] in 2007 used inviscid Cartesian-mesh methods to simulate free and forced oscillation tests of bodies in order to extract the damping characteristics. This was first applied to slender bodies [37] and then extended to the blunt body shapes of Viking, Genesis, and MER [38]. In [37], both a time dependent and a more computationally efficient reduced frequency approach were examined for missile and fighter aircraft shapes. Moderate agreement with experimental data and between methodologies was found, demonstrating the potential for use of computational methods as well as the possibility of using a more cost efficient approach than a purely time dependent scheme. In [38], the

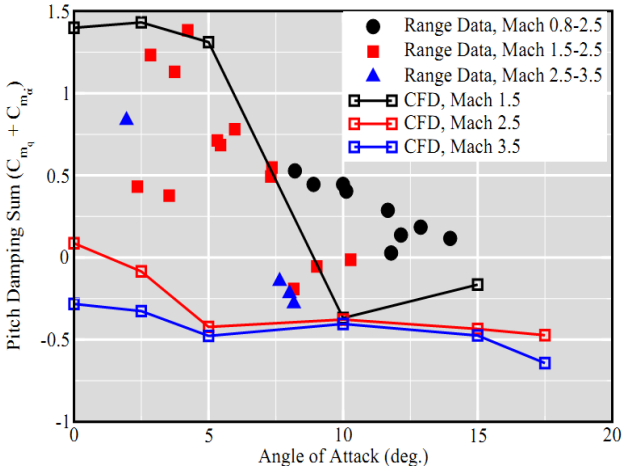

Figure 13. CFD and ballistic range results for MER [38]

time dependent approach was extended to blunt bodies, and results were in moderate qualitative agreement with experimental data (Fig. 13). Additional fidelity was incorporated into the method by Murman in [39] with viscous, Reynolds-averaged-Navier-Stokes (RANS) free oscillation simulations (using the Overflow solver) of the Orion crew module and an inflatable aerodynamic decelerator (IAD) shape. Again, moderate agreement with the available ballistic range data was found (Fig. 14).

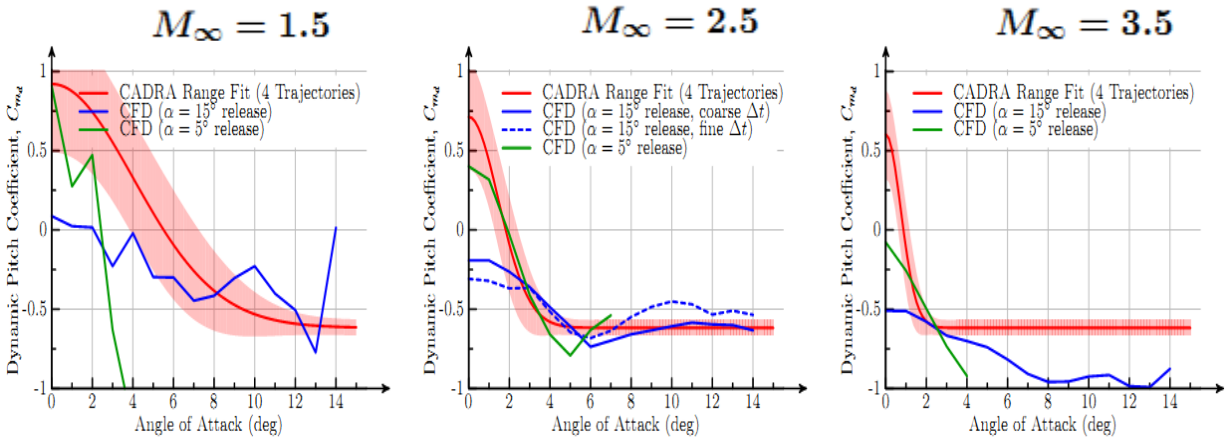

Figure 14. CFD and ballistic range results for IAD configuration [39]

A key observation of this work, however, was the dependence of the CFD results on the initial release angle of attack for the free oscillation simulation. This can be seen in Fig. 14 as the initial angle of attack at release is changed from 5^o to 15^o. As the initial angle is increased, the pitch rate at which the body passes through any particular angle of attack also increases. During the dynamic pitching motion, the pressure field on the aftbody lags the motion of the oscillating forebody (this process and its importance to the dynamic stability phenomenon will be elaborated on in later sections) [19],[39]. The magnitude of the time delay is dependent on the pitch rate of the body, and thus it is suggested that the assumption within the post processing techniques of ballistic range data that the dynamic coefficients are independent of pitch rate should be reconsidered [39].

The most recent CFD work in this area was conducted by Stern et al [40] using dynamic simulation with the flow solver FUN3D which allow for active grid deformation as the body rotates with up to six degrees of freedom. Their results were for a single degree of freedom, free oscillation simulation of the MSL entry vehicle using both inviscid and viscous simulations. The inviscid results were able to predict static aerodynamic coefficients which agreed well with experiment. Moderate agreement between the simulation and experiment was found for the value

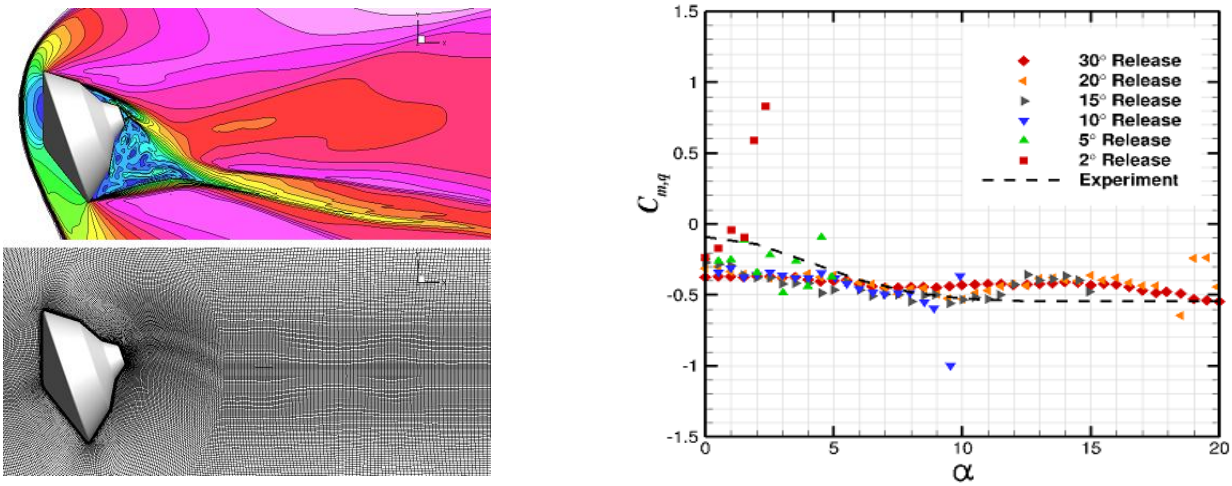

Figure 15. Contours of constant Mach number and the associated grid deformation at α=20^o (left) and viscous results for the pitch damping coefficient (right) at Mach 3.5 [40]

of the pitch damping coefficient for a Mach number of 2.5 and the small angles of attack at Mach 3.5. Error was attributed to the inviscid modeling and the assumptions within the modeling of the aerodynamics and the damping, in particular their lack of dependence on the angular rate.

Preliminary results for the viscous simulations showed significant promise, with much better agreement for the Mach 3.5 case. Although these improvements come at an increased computational cost, continued work with this particular methodology could yield significant contributions to the modeling community and the fundamental understanding of blunt body dynamic stability.

C. Summary

In general, existing computational techniques are insufficient for accurate characterization of a blunt vehicle's dynamic performance, lacking the quantitative accuracy necessary for any analysis beyond the preliminary design stage. An additional limitation of the methodology is the reliance on estimation techniques to obtain the pitch damping (similar to those used for ballistic range tests). As with the experimental methodologies, the shortcomings in the predictive capabilities of empirical or computational techniques stem from a general lack of understanding regarding the dynamic stability phenomenon.

IV. Vehicle Design Parameters and Dynamic Stability

Through the aerodynamic investigations which have been carried out over the last half century, it has become clear that vehicle design parameters have a significant influence on the resulting dynamic response of the body. The highly coupled nature of these effects has made it difficult for researchers to isolate and fully understand the individual contributions of the vehicle parameters on the observed dynamic behavior. In this section, a summary of observations regarding several key vehicle parameters will be presented. From this, further insight will be gained regarding the underlying physical phenomenon of dynamic stability.

A. Center of Gravity Location

With the intuition gained from static stability experiments, one of the first trade studies regarding dynamic stability involved varying the location of the center of gravity. Buell and Johnson [7] investigated this effect in two blunt bodies, one a 30^{o} sphere cone and the other having a parabolic forebody, and found no conclusive trend regarding the damping characteristics as a function of center of gravity location and angle of attack at subsonic speeds. Ericsson presented supersonic results in [29] for the same sphere cone configuration of Buell's study and found that the amplitude and angle of attack range of the instability region decreased as the CG was moved axially toward the nose. Ericsson attributes this behavior to a decrease in the adverse effects of flow separation and reattachment on the aftbody that accompany the forward movement of the CG, outweighing the lengthened lever arm for the aftbody pressure forces to act. In this case, improved static and dynamic stability are both obtained by making an alteration to the vehicle. For most other parameters investigated, however, making changes in order to improve dynamic stability characteristics come with the consequence of reducing static stability.

Other studies [41]-[45] conducted at transonic or supersonic speeds over the years have also concluded that damping improves as the CG is shifted forward. In [42] and [43] it was observed that although moving the CG forward improved damping at low angles of attack, the effect lessens and a more rearward located CG may improve damping at higher angles of attack (Fig. 16).

In some studies, such as that by Uselton, Shadow and Mansfield [41], moving the CG rearward at a Mach number of 3 had a much less pronounced effect than at transonic and lower supersonic Mach numbers. This may indicate that sensitivity to CG location increases as Mach numbers approach the low supersonic, transonic and subsonic regimes as a result of the more prevalent pressure forces in the near wake as flow speed around the corners decreases, allowing for earlier reconvergence of the flow and more substantial near wake and recirculation regions.

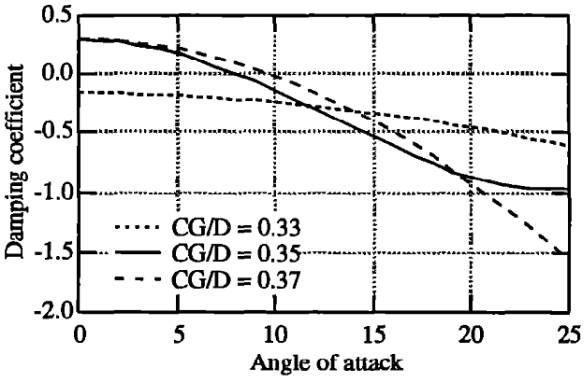

Figure 16. Pitch damping coefficient of the Stardust capsule for various CG locations at M=2 [42]

B. Roll Rate

Inducing a rolling motion on a blunt vehicle during entry can improve static stability characteristics in the pitch and yaw directions. The effect of roll rate on the dynamic response appears to be an area of great need in the literature. Prislin and Jaffe [43] performed analytical and numerical studies which indicated that for a body that is inherently dynamically stable (i.e. has a negative ξ), higher roll rates in the terminal regime of the trajectory amplify the effect of this stability and oscillation amplitudes will be dampened out more quickly. Conversely, for unstable bodies (with a positive value of ξ), the amplitude of oscillation will damp out more slowly prior to maximum dynamic pressure and diverge more quickly afterward as the roll rate of the body increases.

Later, Jaffe [44] performed drop tests in the Vehicle Assembly Building of various blunt sphere cone bodies in order to study this phenomenon experimentally. By fitting trajectories through the observed histories of angle of attack versus time, estimates for the pitch damping sum were obtained. By looking at Fig. 17, it can be seen that the results agreed with the analytical predictions of the previous work in finding that damping increased (favorably) as

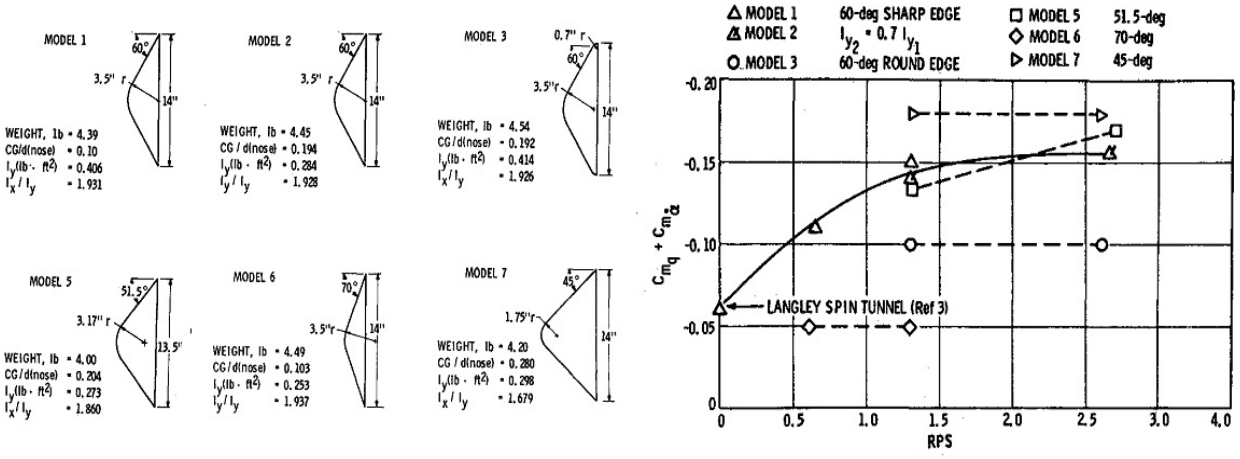

Figure 17. Models used (left) and summary of results (right) from drop test study [44]

roll rate increased. It must be noted, however, that this experimental study suffered from airspeed limitations (as do similar methods like vertical spin tunnels) and was only conducted at Mach numbers on the order of 0.05. The work of [43] provides motivation to investigate this effect at earlier (and more relevant) portions of the trajectory where higher roll rates indicated slower convergence.

C. Forebody Cone Angle

The effect of forebody cone angle on dynamic stability characteristics has had some contradictory results throughout the literature. In general, authors seem to believe that decreasing cone angle improves the dynamic response of the vehicle. This was cited in much of the early work in the late 1960's and early 1970's [41]-[45] at low subsonic, transonic and low supersonic Mach numbers. Forced oscillation data from tests by Uselton, Shadow and Mansfield [41] are reproduced in Fig. 18 and show clearly that the 60° half angle sphere cone has a more favorable damping coefficient across multiple Mach numbers and angles of attack, with the effect being more pronounced at zero inclination to the flow (α=0°). This sentiment about the effect of cone angle has also been cited in more recent studies, such those regarding the Mars Microprobe mission by Slimko et al [46] where the authors

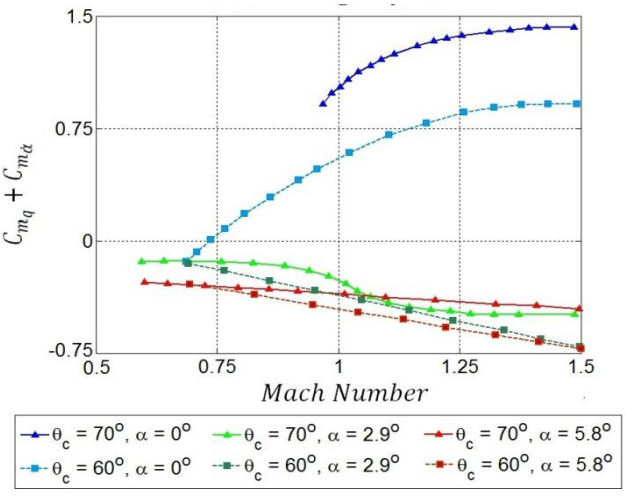

Figure 18. Effect of cone angle on the damping of 60° and 70° sphere cone vehicles [41]

recommend using a minimum cone angle for improved dynamic stability. They go on to cite the physical reasons for this observation, suggesting that the sharper geometry will help to reduce the size of the separation region near the aftbody and reduce the pressure fluctuations on the body due to changes in angle of attack.

The contradictory results come from the thorough free oscillation experimental investigations by Fletcher [4],[5] regarding the effect of geometric changes on the dynamic stability behavior of various bodies. Two of the geometries he tested were sphere cones of equal nose radii and CG location, but with cone angles of 10^o and 19^o. His results (obtained at $\alpha=0^o$) show the exact opposite trend as the observations discussed previously. Across mi subsonic, transonic and supersonic Mach numbers, he found the 19^o body to be consistently more stable. The data from this study and schlieren photographs at M=2.91 of both bodies are shown in Fig. 19. Directly conflicting results such as those between Fig. 18 and Fig. 19 emphasize the unpredictable nature of dynamic stability and the general lack of understanding about the nature of the phenomenon. Inconsistencies in the results may also have to do with differences in testing methodologies: Uselton et al [41] obtained their results using forced oscillation, Fletcher [4],[5] a free oscillation setup, and Marko [45] a free flight wind tunnel. Additionally, results in which cone angle is isolated entirely (as Fletcher was able to achieve) are not easily found. Marko [45] notes that in his study, and effects of cg location and corner radius may be contributing factors to the observed stability trends. Finally, the models used by Uselton et al [41] differed in nose bluntness and slightly in the CG location.

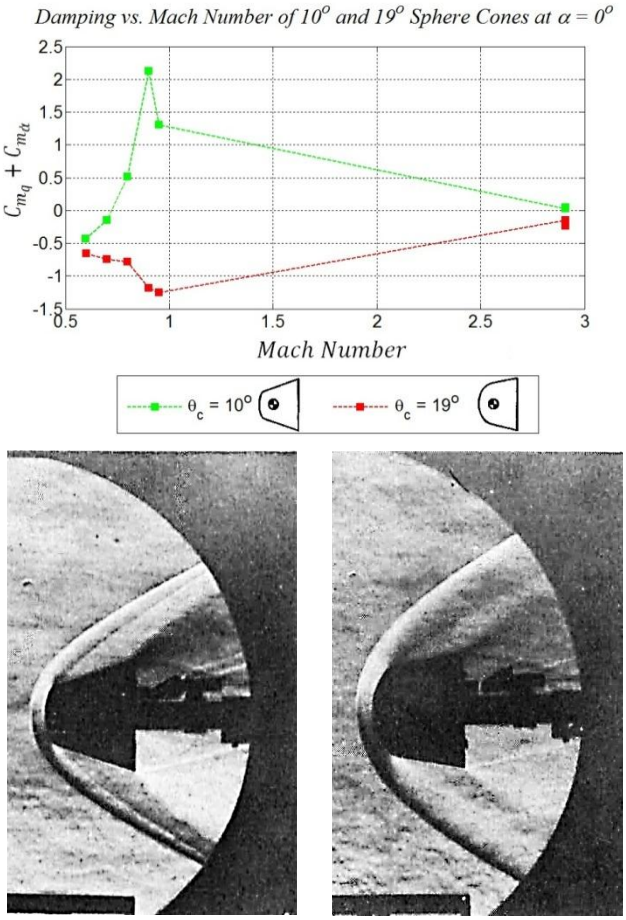

Figure 19. Effect of cone angle on damping (top) and flow characteristics (bottom) [adapted from [4],[5]

D. Nose Radius

The early conclusion by the groundbreaking work of Allen and Eggers [47] found that aerodynamic heating considerations require entry vehicles to be blunt. The consequences of this geometric design constraint on dynamic stability have been looked at by several studies. The comparative geometries from two of these studies conducted by Fletcher [4],[5] are compiled in Table 2. His results found this decrease in stability as the nose radius was decreased at both sub and supersonic Mach numbers. For both a conical section body and a Mercury-like body, his results showed that the more slender configuration (that with the smaller nose radius) was less dynamically stable. For the Mercury configurations, the effect disappeared when the Mach number was increased from 2.2 to 2.91, indicating a possible heightened sensitivity to the effect as the Mach number approaches the critical regime near Mach 2 where instabilities typically arise.

Table 2. Effect of Bluntness

Study	Larger Nose Radius Configuration	Smaller Nose Radius Configuration
Fletcher [4],[5]		
Fletcher [5]	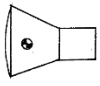	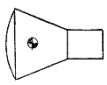

Although intuition may seem to indicate that the slender body should be more dynamically stable, there are other results presented by Ericsson [49] that show similar improvement in stability with blunted nosed cones relative to

sharp cones. Separating bluntness effects from those of shoulder radius, cone angle, and general vehicle shape is often difficult, but the simple geometries and modifications used by Fletcher were the quite effective in doing so.

E. Shoulder Geometry

Low subsonic drop tests by Jaffe [44] indicated a slight decrement in stability performance for sphere cone bodies having rounded shoulders (shoulder radius 5% of maximum diameter) compared to that of a sharp configuration. Transonic studies by Krumins [48] and Sammonds [50] noted no noticeable difference for near identical forebody configurations and shoulder radii. Fletcher's [4] results for flat faced, expanding 10^o conical sections in subsonic flow noted significant improvement in stability performance when the corners were rounded to 10% of the maximum diameter. However, this effect was not present when he tested identical models at a Mach number of 2.91 [5]. Also, when contracting conical sections were examined for the same effect, it was found that rounding the corner to 15% also improved subsonic stability, although to a lesser extent than the expanding configuration.

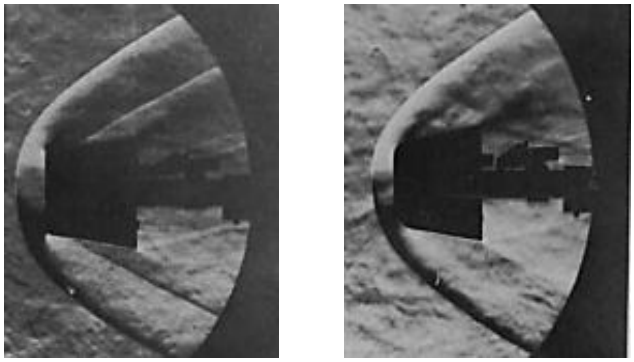

Figure 21. Schlieren images of the 10^o conical sections with sharp (left) and rounded (right) corners at M=2.91 [5]

Having a sharp shoulder provides a discontinuity that provides a fixed separation point for the flow as it accelerates over the body. Schlieren images of Fletcher's M=2.91 test shown in Fig. 21 demonstrate this effect. The flow features downstream of the bow shock are more defined for the sharp cornered body relative to those for the body with the rounded shoulder. Taking this into consideration, it is possible that the environment behind the sharp body would experience less temporal variation and thus less pressure variation on the aftbody to induce instabilities. This hypothesis would coincide with Jaffe's results. Conversely, if the recompression shock were strengthened due to the pressure of a steadier flow field, the recirculation region behind the body may actually see stronger pressure fluctuations through the interaction between the recompression shock and the base flow. This mechanism was proposed by Teramoto [19].

Given the previous discussion, we see that conflicting conclusions could be drawn regarding effect of corner radius on the dynamic response, depending on the interpretation of the resulting flow structure.

F. Boundary Layer Trips

In addition to using a sharp shouldered geometry to create a fixed separation point, the use of "roughness strips" on the forebody to trip the boundary layer and induce separation was investigated by Wiley et al [52] and then reexamined by Ericsson [29]. With the hypothesis that the separation and reattachment of the flow over the body were the cause for the erratic dynamic behavior, Ericsson used the roughness strip as a means to isolate this effect. Fig. 22 shows the effect of the roughness strip at transonic speeds for a sphere cone vehicle. It can be seen that subsonically, the roughness strip drastically increases the damping parameter (and thus reduces dynamic stability). Above M=1.1, however, the trend reverses and an improvement in stability is seen with the addition of the roughness strip. These trends provide insight into the underlying mechanism causing dynamic instabilities.

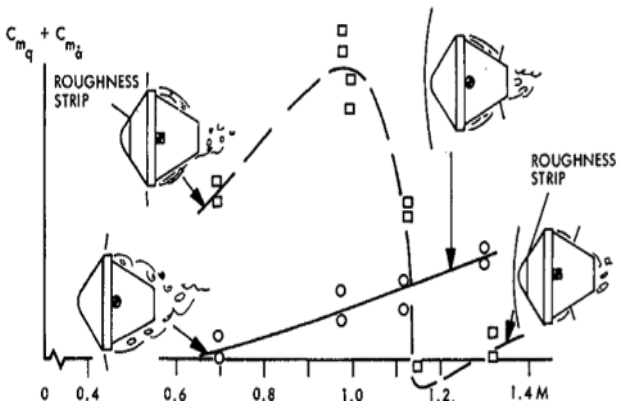

Figure 22. Effect of forebody roughness [29]

It is theorized that, at subsonic and transonic speeds, the separation and subsequent reattachment of the flow on the body resulted in reduced dynamic stability (and increased static stability). For the configuration and test conditions for the results in Fig. 22, the flow remains attached to the "smooth" body when the flow is subsonic and

thus the decrement in stability due to reattachment is not realized, as it is when the flow is tripped with the roughness strip. At supersonic speeds, both vehicles experience separation and reattachment. The body with the roughness strip, however, causes earlier separation and reattachment. The consequence of the reattachment occurring further aft for the smooth body is a larger moment due to the unsteady pressure forces and thus reduced dynamic stability, relative to the vehicle with the roughness strip.

G. Aftbody Effects

Since the earliest investigations into blunt body dynamics, researches have noted the significant dependence of the observed response on the aftbody geometry of the vehicle. Several studies have applied modifications to the aftbody to investigate how design choices impact the resulting dynamic stability characteristics a vehicle. The results collected from a wide array of modifications have cemented the early findings about the significance of this design choice, helped establish favorable configurations, and shed light into the underlying physical mechanism which govern the phenomenon.

1. Presence of an Aftbody

The influence of the presence of an aftbody on dynamic stability has been studied by several authors. Buell and Johnson [7] and Beam and Hedstrom [8] tested for this effect on 30^o sphere cone and parabolic shaped bodies at subsonic and supersonic conditions, respectively. The papers by Bird [3] and Ericsson [29] looked at these results further. All of the authors came to the conclusion that the presence of an aftbody greatly affects the resulting dynamic response of a body. The top plot in Fig. 23 combines the data from [7] and [8] to demonstrate this clearly. The presence of the aftbody decreases damping for all Mach numbers investigated, with the effect being more pronounced at lower Mach numbers for the parabolic body and consistent across all Mach numbers for the sphere cone with the small aftbody. When the aftbody size was increased for the sphere cone at M=2.5 the detrimental effects seem to be greatly reduced. Looking at the lower plot in Fig. 23 the effect of angle of attack is demonstrated. Alone, the sphere cone forebody is approximately neutrally stable between -1^o and 1^o while the vehicle with the aftbody is highly unstable at these low angles of attack. As the incidence angle increases, however, the vehicle with the aftbody becomes stable and the damping sum of the forebody alone configuration drifts further positive and becomes unstable.

2. Length of Aftbody

Volumetric requirements and packing considerations typically require that an entry vehicle have an appreciable aftbody. With the knowledge that the effects of an aftbody on dynamic stability are generally undesirable, modifications to the length of the aftbody were investigated. This effect was of particular interest for the manned vehicles that had long aftbodies due to their packaging requirements. Igoe and Hillje [11] removed the antenna and parachute canisters from the aft portion of the converging conical aftbody of the Mercury capsule, thus reducing the axial protuberance length of the aftbody in the trailing flowfield. This was shown to be detrimental to the dynamic stability as the basic configuration had significantly greater damping (a more negative damping coefficient) for low and moderate angles of attack at Mach numbers between 0.3 and 1.2. The removal of the aftbody features in the near wake may intuitively seem to improve dynamic stability because of the reduced lever arm. The exact reason for the observed behavior is not known, but Baillion [13] cites the location of flow reattachment as being dependent on both the angle of incidence and the axial length of the typically conical aftbody. As the reattachment and the flowfield associated with it are both unsteady phenomena, it is not unexpected that the

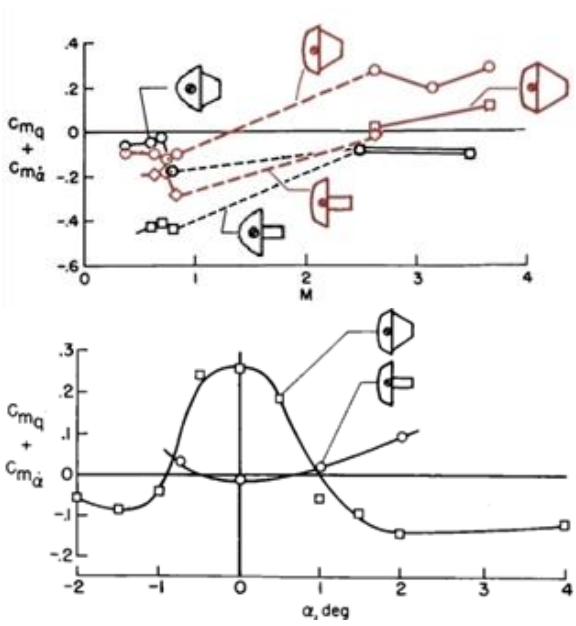

Figure 23. Effect of an aftbody on damping with Mach number (top) and angle of attack (bottom) [7],[8]

removal of the canisters would greatly alter the damping behavior.

3. Aftbody Flare

Another aftbody geometry modification which was investigated was referred to by Fletcher [4],[5] as "pinching the waist" of the body. This resulted in an aftbody geometry which was convergent aft of the maximum diameter location until it reached a point further aft, when the slope would change such that the aftbody began expanding, effectively introducing an aftbody flare. The effects of the flare on the resulting flow structure for a sphere cone body and the Mercury capsule were captured by Fletcher and Wolhart [5] and are shown in Fig. 24. The additions of the flares to both bodies significantly decreased dynamic stability. By looking at the supersonic flow structure, some key features can be identified which indicate that this result is not an unexpected one. As is typical, the contraction aft of the shoulder for both the flared and unflared bodies results in expansion waves and a separated recirculation region. When the flare is added, the shear layer impinges on the expanding surface. This is a highly unsteady phenomenon and the interaction between this shear layer, the unsteady pressure forces in the recirculation region which it encapsulates, and the shock structures aft of the pinched location results in a flow environment which is highly time variant. For the sphere cone, moving the pinch from 79% of the axial length of the body up toward the nose to an axial position of 54% of its length eliminated the instabilities caused by the flare and exhibited the same dynamic response characteristics as the unflared body.

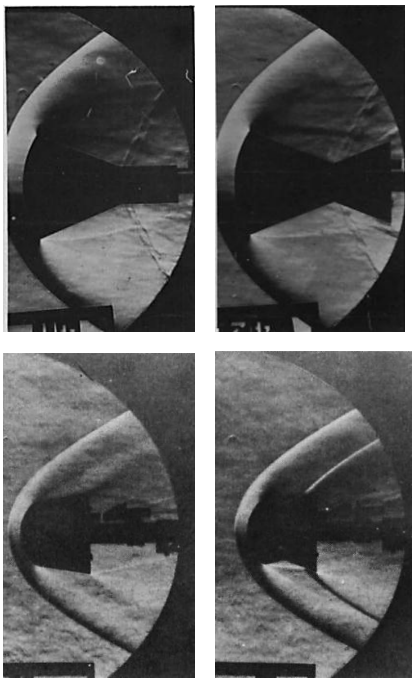

Figure 24. Flow modification due to an aftbody flare (M=2.91) [5]

When the same sphere cone configurations were tested at subsonic speeds by Fletcher [4], it was discovered that the observed effects of the flare were opposite of those found supersonically. For Mach numbers between 0.6 and 0.9, the unflared body was dynamically unstable, but adding the pinched waist made the vehicle stable in this regime. Furthermore, the more forward location of the flare, which had no noticeable affect supersonically, was found to be the most favorable geometry subsonically, substantially better than the rearward flare. The stark contrast between the observed subsonic and supersonic influence of the flare indicates that the flow structure must differ significantly between these two regimes and the manner by which the pressure forces in the resulting wake manifest into dynamic oscillations depends heavily on the free stream conditions.

Fletcher also [4],[5] looked at the effects of adding fin structures circumferentially on the aftbody. Similar to the flare studies, it was found that at subsonic speeds the fins improved stability; however, at supersonic speeds the effects were negligible. Finally, the rocket nozzles protruding from the aftbody of the BLDT test configuration of the Viking vehicle were shown to improve damping by a factor of two at zero angle of attack, but had negligible effect at nonzero inclinations [21].

4. Spherical Aftbody

The most critical and insightful investigations into aftbody geometric variations focused on the effects of adding a spherical segment aft of the shoulder. Wehrend in 1963 [12] examined this effect for slender sphere cones with the center of curvature in three different locations: aft of the CG, coincident with the CG, and forward of the CG. His results showed that the flat based configuration was more dynamically stable than all of the bodies having spherical sections on the aftbody. As the center of curvature of the spherical base moved forward, the detrimental effects of were reduced. Ericsson [29] addressed similar slender configurations and noted the same undamping effect. Since the forces generated on the spherical aftbody cannot generate any pitching moment when the center of rotation is coincident with the CG, he attributed the observed effects to the enhancement of the aftbody wake response to flow changes on the forebody by "facilitating" communication through the boundary layer between the forebody and aftbody. This effect is much more pronounced at subsonic and transonic speeds because when the flow is supersonic, upstream communication can only occur in the subsonic portion of the boundary layer. Interestingly, Ericsson noted that the observed effects reverse, i.e. the rounded base is favorable, if the forebody geometry is such that the lift derivative is negative, thereby causing the wake (and the induced loads associated with it) to be "inclined opposite to the angle of attack."

Sammonds [50] conducted a study on a vehicle with a 60^o sphere cone as the forebody that seems to substantiate the hypothesis of Ericsson. By adding a full-diameter hemispherical section whose center of curvature was coincident with the body's center of gravity, he removed any possible moment contribution that could be generated by the unsteady aftbody pressure field. His results (Fig. 25) show that this alteration fully eliminated the instabilities, which were seen from the forebody alone configuration, and the modified vehicle was stable for all angles of attack. The improved stability and reduced non-linearity of damping behavior for blunt vehicles utilizing a spherical aftbody was also seen in the development of other blunt atmospheric entry probes. Slimko et al [46] and Mitcheltree et al [51] cited this aftbody modification as one of the key factors for improving dynamic stability for Mars Microprobe, with Slimko et al [46] noting that the viscous forces along the spherical segment act in the direction opposite the direction of rotation, thereby increasing damping. Chapman et al [53] presented results from Mars Microprobe and Huygens, noting that in addition to ensuring that aftbody pressure forces act through the CG and thus cannot generate pitching moments, the spherical aftbody also modifies the nature of the separation of the flow at the shoulder, reducing the size of the expansion and recirculation regions.

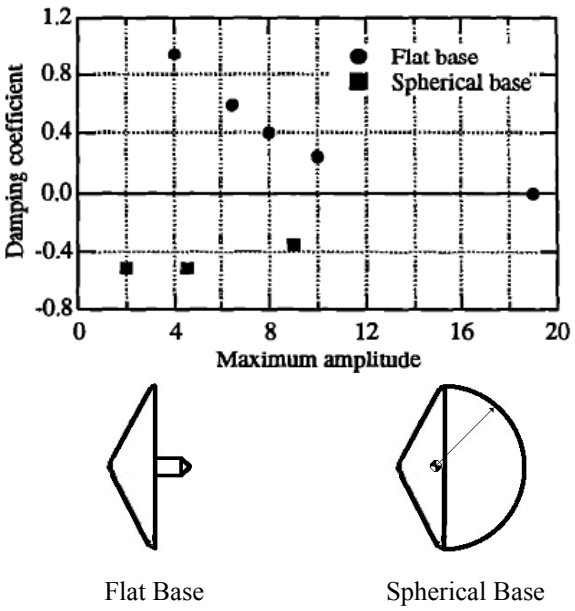

Figure 25. Effect of spherical base on damping behavior [50],[53]

To investigate the effects of the spherical base further, Chapman et al [53] conducted a computational investigation of wake features using steady state CFD to better understand the mechanism by which the spherical aftbody alters pitch damping. These solutions indicated that the spherical aftbody causes the shear layer of the flow and the location of the recompression point within the wake to migrate closer to the body. As Mach number is increased from the transonic regime to the mid supersonic regime, these effects are magnified. The authors compared these observations to shadowgraphs of the flowfield and noticed substantial differences in the predicted features relative to experiment. The experimental flow separated sooner and reconverged much less quickly than the CFD solutions indicated. These stark differences highlight the deficiencies in steady state computational tools to capture critical time dependent effects of the complex flow in the wake of a blunt body.

V. Environmental Parameters and Dynamic Stability

As with the vehicle design parameters, the literature reveals that blunt body dynamic stability is highly sensitive to environmental parameters. Given the coupled nature of many of the flow conditions, effects of individual parameters are difficult to isolate with the available test facilities.

A. Mach Number

The effect of Mach number is dependent on the configuration being studied. Hypersonically, damping exhibited remains relatively constant with Mach number and is typically stable or neutrally stable. Between the hypersonic and subsonic regimes, the damping begins to decrease and the body generally becomes unstable, with a peak in the instability usually occurring between Mach 3 and Mach 1. As the vehicle approaches the transonic regime, a second instability spike is often found and then the damping increases again as the vehicle decelerates through subsonic speeds. This behavior results in an oscillation envelope history that converges gradually towards zero from atmospheric interface down to high supersonic Mach numbers, after which it begins to grow rapidly through the transonic regime until it converges again subsonically. The trends described above can be shown using several representations. When using ballistic range data, it is typical for the damping coefficient to be plotted against angle of attack for several different Mach numbers. Using this damping coefficient behavior obtained experimentally, the oscillation amplitude history as the vehicle decelerates can be plotted versus time (and Mach number). Experimentally obtained damping results from Schoenenberger [54] and the corresponding simulated oscillation history investigated by Smith [55] for the Mars Science Laboratory vehicle are shown in Fig. 26. This practice and

the resulting depiction of the results provide engineers and mission planners with valuable information regarding the state of the vehicle throughout the trajectory, particularly for the key parachute staging event.

Insight into the reasoning for the critical Mach number at which dynamic instabilities typically arise can be

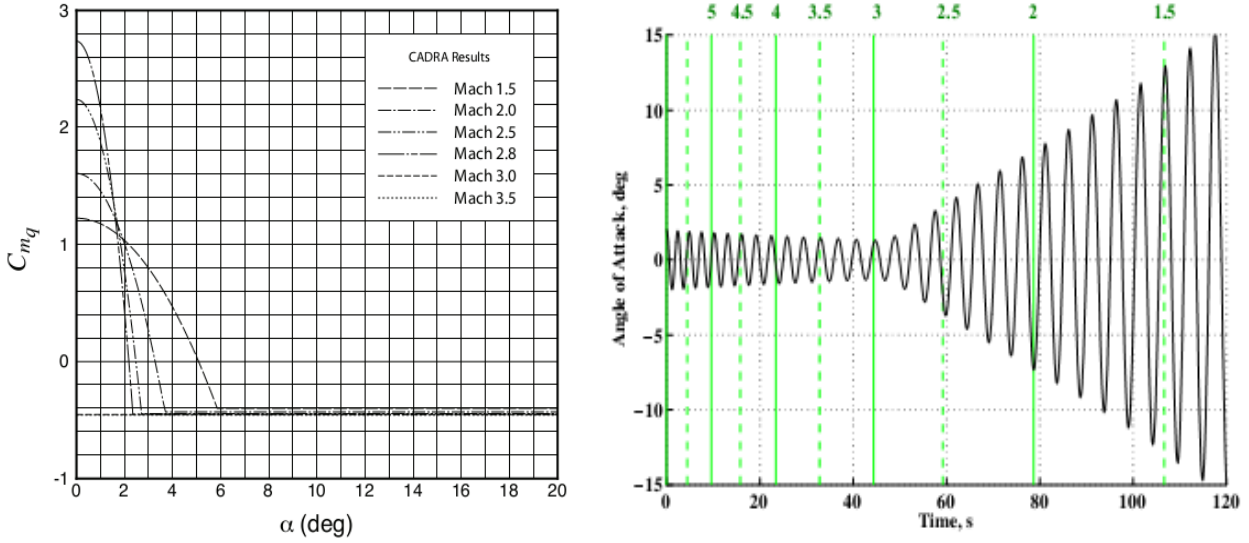

Figure 26. MSL damping coefficient versus angle of attack at various Mach numbers (left) [54] and simulated oscillation history with vertical lines indicating Mach number (right) [55]

obtained from looking at wind tunnel data obtained by Clark [56] during his wind tunnel investigation of a tension cone shaped entry vehicle. His data showed that as the vehicle decelerates at Mach numbers of 2.5 or greater, the aftbody pressure coefficient decreases at a faster rate than the forebody pressure coefficient. Below Mach 2.5, however, the trend reverses and the forebody pressure coefficient begins to decrease at a rate greater than the aftbody pressure coefficient. The Mach number at which this crossover occurs is at the point where instabilities are typically greatest for blunt bodies, pointing to the possibility that the relative rate of change between the forebody and aftbody pressure coefficients may be critical to the onset of dynamic instabilities. As the forebody pressure coefficient begins to decreases faster than the aftbody, the relative contribution of the aftbody pressure and the resulting oscillation behavior increase, resulting in decreased damping. This is consistent with intuition given the importance of the aftbody pressure field on dynamic stability.

B. Reynolds Number

The effect of Reynolds number has been looked at thoroughly in the literature with inconclusive and contradictory observations. Negligible influence has been noted for various geometries over the decades at a range of conditions.

Most troubling about the contradictory results summarized above, is the fact that when Reynolds number dependence was observed, it not only altered the magnitude of the damping significantly, but also the general behavior with respect to Mach number and angle of attack. Fig. 27 plots the results from the Stardust [57] and Orion [20] studies (note that although Orion uses the Apollo definition of angle of attack, the x-axis was shifted to the more traditional definition used by Stardust for consistency in comparison). In [20] it was recommended that subsequent tests be tested nominally above Reynolds numbers of 5.0 x10^6 and not below 3.0 x10^6 to avoid the dependence of the results on Reynolds number.

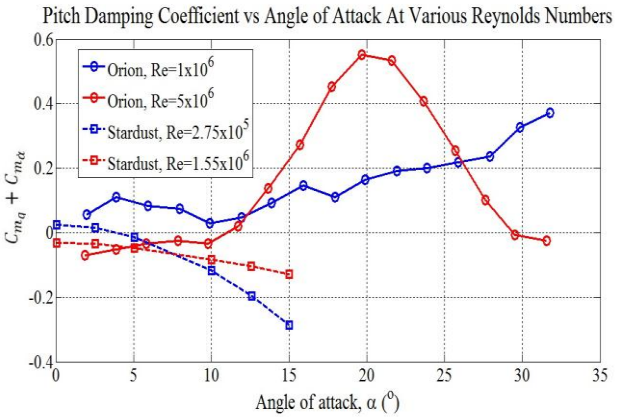

Figure 27. Effect of angle of attack for Orion [20] and Stardust [57] (adapted)

Given the conclusions earlier in this report regarding the sensitivity of the dynamic response to the

transition characteristics of the flow, it is possible that the Reynolds number effect is coupled with the geometric variables of the vehicle under consideration. As Reynolds number changes, the location and degree of the flow separation as well as the properties of the boundary and shear layers may change.

C. Strouhal Number (Reduced Frequency Parameter)

Strouhal number (Sr, St, or k), also known as the "reduced frequency parameter," is a nondimensional scaling parameter calculated using the relationship below:

$$k = \frac{2\pi f l}{V_\infty} = \frac{\omega l}{V_\infty} \tag{8}$$

where ω is the angular velocity of the oscillatory motion (in rad/s), l is the characteristic length (diameter for blunt bodies), and V_∞ is the free stream flow velocity. Note that a factor of 2 in the denominator is occasionally used in the literature. This scaling parameter captures the relative magnitude of the frequency content of a body's oscillatory motion to the mean rate at which the free stream flow passes over the body. As the interactions of the resulting flow structure and the aftbody of a vehicle are critical to dynamic stability, matching of *k* during sub scale testing of dynamic behavior is important for estimating limit cycle behavior and identifying any possible resonance frequencies that may be responsible for excitation of pitching oscillations.

Wang et al [59]-[61] studied the spectral characteristics of the flow structure at various locations around an Apollo capsule at low speed. Of particular interest were the oscillations of the rear stagnation point because of their possible influence on unsteady loads acting on the aftbody of the vehicle. Throughout the wake, frequency signatures were detected corresponding to reduced frequencies of 0.08 and 0.16. The authors theorize that these structures were related to the shedding and meandering of vortices in the near wake. Other spectral signatures were found in the flow, but their physical significance could not be identified. Although their studies were done at subsonic and transonic speeds, they postulate that the flow structures identified would be similar enough to be used for characterizing the dynamics at higher Mach numbers. Murman [37] used this same idea to develop a computational method for predicting damping with reduced computational cost.

Experimentally, a few studies that considered the effect of the reduced frequency parameter found a correlation between its value and the observed damping. The BLDT configuration of the Viking vehicle was found to be highly sensitive to reduced frequency at various Reynolds numbers and a Mach number of 1.76. Interestingly, their results indicate the strongest influence at a Strouhal number of 0.016 (Fig. 28, note the authors utilize the factor of two in the denominator in their definition), an order of magnitude less than the dominant frequencies found in the studies by Wang [59]. Similarly, Teramoto [19] cited the Strouhal number of the Muses-C capsule as 0.03. This may indicate that the frequency content of the flow features in the wake of a blunt body is sensitive to changes in vehicle geometry or that extending the incompressible measurements to higher Mach numbers should be avoided.

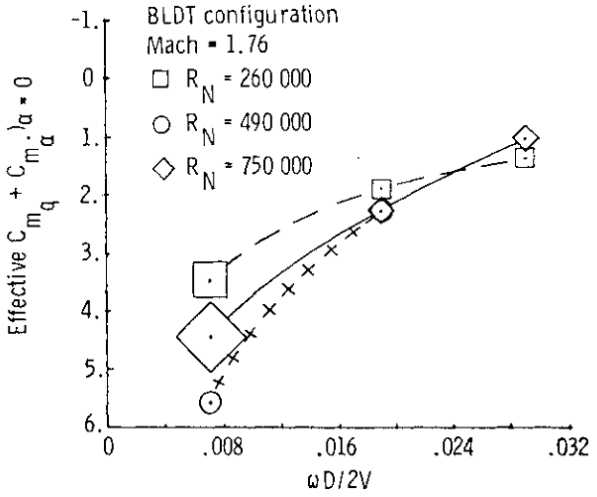

Figure 28. Effect of reduced frequency parameter on damping of BLDT vehicle [21]

D. Specific Heat Ratio

For missions with destinations to bodies with atmospheres unlike our own - Mars, Venus, Titan, etc. – it is often challenging for dynamic test facilities to match the test gas with one that is representative. Chapman and Yates [23] note that although the issues associated with chemically reacting flow are typically no longer of concern in the supersonic regime where dynamic stabilities are most prevalent, the effect of the specific heat ratio of the medium on the resulting dynamic behavior can still be important. It has been observed that surface pressure distributions and shockwave geometry are dependent on the specific heat ratio [48],[62],[63]. Given that the unsteady interactions of

pressure fields and shockwaves could possibly excite dynamic instabilities, there exists a clear means through which the specific heat ratio could modify dynamic stability.

Krumins [48] quantified this effect by comparing the damping measured in air (γ = 1.4) and Tetrafluoromethane (CF_4, γ = 1.12) for bodies with sphere cone, spherical section, and tension shell forebodies. Shadowgraph images of the tension shell in Fig. 29 exhibit drastically modified shock structure with the change in test gas. For the sphere cone, tests in air revealed a stabilizing damping coefficient while tests in CF_4 found the same configuration to be dynamically unstable. This points to the composition of the medium as a possible reason for the higher than predicted oscillation growth that has been observed on missions such as Mars Pathfinder [54]. Given the exploration interest in bodies such as Mars and the potential implications of under predicting damping by testing in ground facilities utilizing air, further understanding of this phenomena and development of facilities with variable test gas capabilities may benefit the community greatly.

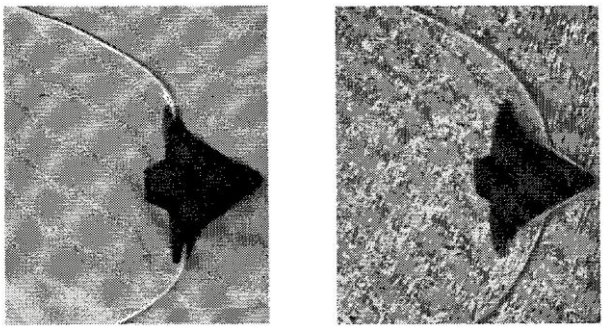

a) CF_4: $M = 6.6$; $R_d = 1.82 \times 10^5$ b) Air: $M = 6.1$; $R_d = 0.73 \times 10^5$

Figure 29. Shockwave shapes for a tension shell in CF_4 and air [48]

VI. Physical Mechanisms

Understanding the possible physical mechanisms that govern the vehicle's dynamic response would aid in reducing uncertainty. As is pointed out by Abe et al [67], descriptions of both the oscillation growth and the subsequent limit cycle behavior lack a fundamental understanding. This section will highlight the few proposed explanations that exist in the literature and provide further insight to the phenomenon of dynamic stability.

A. Pitching Moment Hysteresis

Early investigations of blunt body dynamics showed that a negative correlation existed between the trends of the static and dynamic stability coefficients. Beam and Hedstrom [8] noted that small changes in the static stability derivative (C_{m_α}) corresponded to opposing changes in the pitch damping coefficient, $\left(C_{m_q} + C_{m_{\dot{\alpha}}}\right)$. This observation led to a theory that suggested the direction of the pitching motion causes nonlinearities in the pitching moment slope due to the finite time delay that exists between changes in pitch angle and subsequent changes in the pressure field over the body. This hysteresis effect has been cited by other studies seeking to describe the mechanism behind dynamic stability. It has been concluded both experimentally [68] and numerically [19] that the

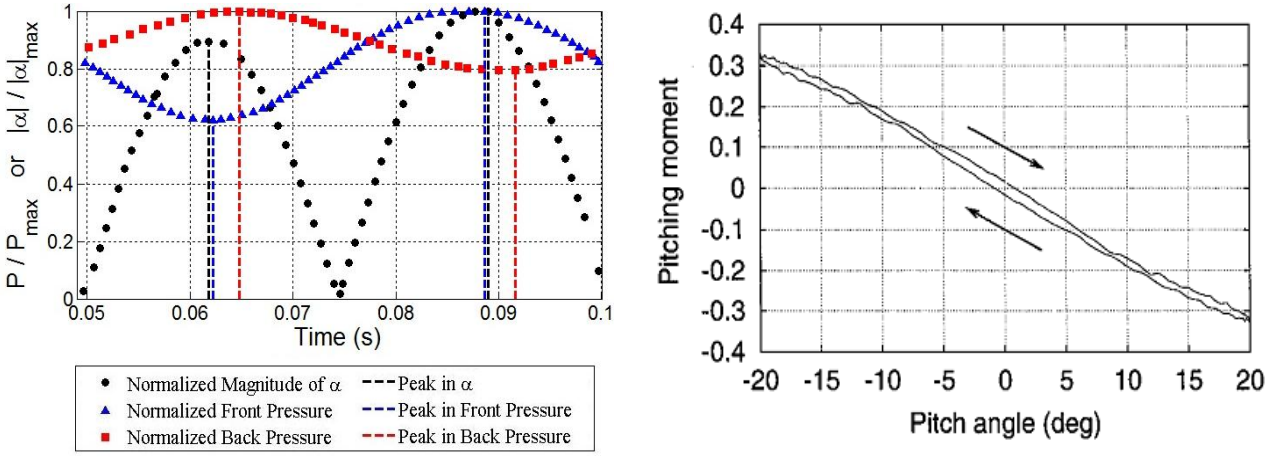

Figure 30. Pressure variation with pitching motion (left) and corresponding hysteresis in pitching moment (right) [19]

aftbody pressure field lags the pitching motion and changes in the forebody pressure. Fig. 30 presents numerical simulation data from [19] that demonstrates this delay and the resulting pitching moment hysteresis. While the peaks of the forebody pressure follow closely in time to the peaks in angle of attack (i.e. pitch angle), the aftbody pressure responses lag the oscillation peaks. It is thought that this time delay is the source of the observed hysteresis in the static stability coefficient. The consequence of the hysteresis effect is a net input of work from the flowfield into the pitching motion of the vehicle over each oscillation cycle.

Analytical predictions of this cyclic work input were developed first in [8] and later in [67]. Eqn. (9) shows that the work over one period of oscillation is a function of the dynamic pressure, the reference geometry, and the integral over one oscillation cycle of the pitching moment coefficient. The integral represents the area enclosed by the pitching moment curve such as the one shown in the bottom of Fig. 30.

$$W = \frac{1}{2}\rho V_\infty^2 AD \int_{-\theta}^{+\theta} C_m \, d\theta \tag{9}$$

Positive values of the work over a cycle indicate that the fluid lost energy into the oscillating system and represent a dynamically unstable cycle. If the hysteresis effect were not present, the integral would go to zero over a given cycle and no dynamic excitation would occur. According to this analysis, if the pitching moment curve at a given Mach number encloses some area (moving in the counter-clockwise direction with time, indicated by the arrows in Fig. 30), then the vehicle is dynamically unstable at that condition and divergence will occur. By decomposing the pitching moment for both the front and rear pressure distributions into steady and dynamic components, Abe et al [67] were able to recreate the limit cycle behavior typical of blunt bodies. Their results showed that, by assuming a time delay of twenty times the ratio of D/V_∞ (based on their numerical results), the work integral is positive for values of the pitch angle up to ~20^o, after which it becomes negative. In this case, the oscillations grow (due to positive work input) up to a limit oscillation amplitude, beyond which the damping becomes favorable and prevents further divergence. This behavior and the magnitude of the limit cycle are representative of the dynamic behavior of most entry vehicles studied to date.

1. Physical Explanation for Observed Hysteresis

Given that there exists a proposed means by which a pitching moment hysteresis could result in excitation of dynamic oscillations, significant insight could be gained if one could identify the physical flow phenomena that drive this process. A connection between aftbody pressure fluctuations, the time delay of their response to pitching motions, and the time varying flow structure was proposed by the numerical investigations of Teramoto et al [19]. Using CFD as a means to track time-accurate changes in the flowfield due to pitch oscillations, they were able to identify the features and interactions which could be potential sources for dynamic instability. With this time accurate data, they then looked at the interaction between flow structures within the wake to determine how disturbances due to vehicle oscillations propagated through the system and eventually modified the base pressure of the vehicle, causing the hysteresis effect in the pitching moment that adds energy to the system and drives oscillation growth. As mentioned previously, it is generally accepted within the community that current computational tools cannot accurately predict the pitch damping coefficient which is required for a quantitative assessment of the dynamic oscillation growth. However, the use of CFD to understand the mechanism and trends driving the phenomena can yield insight into the physics. Although experimental verification is required, this explanation is the most physically realistic picture of the possible physical events and their interactions that could be responsible for the dynamic instabilities seen in blunt bodies.

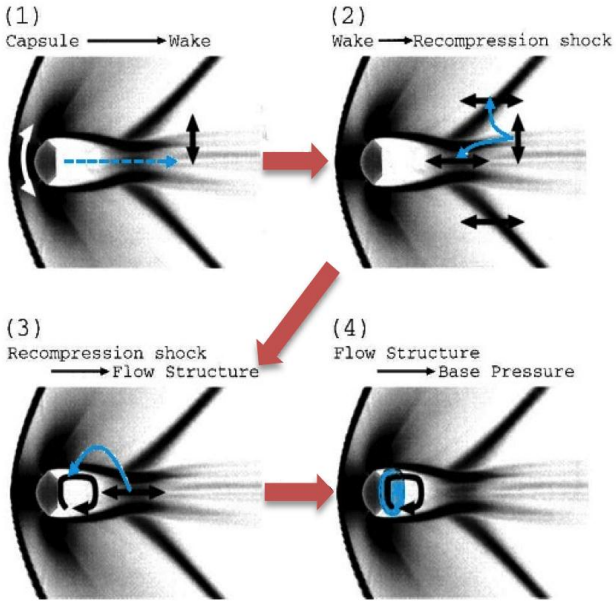

Figure 31. Proposed sequence of events as the mechanism governing dynamic stability [19]

By looking at the phases of the pressure fields outside of and within the recirculation region in the near wake, it was concluded that the base pressure (governed

by the recirculation region) could not be directly influenced by the outer wake through the shear layer. Rather, by tracking at the time varying position of the recompression shockwave and its time delay relative to pitching motions, it was determined that the base pressure fluctuations within the recirculation region were associated with the behavior of the recompression shockwave. Wang et al [60] suggested a similar connection between the oscillation of a body and the "flapping" motion of the rear stagnation point. The behavior of the recompression shockwave seemed to be dictated by the behavior of the wake downstream following the convection of disturbances due to pitch oscillations. Each step within this sequence of events (depicted in Fig. 31): propagation of upstream disturbances due to pitching motion, modification of the wake downstream, motion of the recompression shock, and changes in the flow structure and base pressure within the recirculation region, has a finite time delay associated with it due to finite convection speeds within the flow. Combined, these time delays are responsible for the time lag seen in the base pressure and result in the observed hysteresis in the pitching moment.

B. Flow Separation and Reattachment

Throughout this study it has been clear that the unsteady near wake of a blunt body can greatly affect its dynamic stability. The physical means by which this occurs, as proposed by Teramoto et al [19], was summarized in the previous section. However, this is not the only proposed manner in which the flow structure could generate unsteady dynamic forces. Ericsson and Reding [29] (and later Baillion [13]) cited detrimental effects of flow reattachment on a vehicle following separation off the nose or maximum diameter location. Just as with the near wake effects within the recirculation region, the reattaching flow structures create a closed zone of unsteady pressure forces to act on the rear portion of the vehicle and generate pitching moments. Theory was developed in [29] to predict the induced normal forces that would act on the vehicle and cause instabilities. In applying this method to slender cylindrical bodies with rearward flares, moderate success was obtained in determining damping, although a more descriptive picture for the process and its governing principles is still required for a full understanding of the phenomenon.

VII. Conclusions

After a half of a century of investigation, the phenomenon of blunt body dynamic stability remains one of the least well understood aspects of the atmospheric entry, decent, and landing problem. Analytical and computational techniques to accurately predict the dynamic response of this class of vehicles are inadequate and researchers must still generally rely on experimental methods to estimate the expected damping. Experimental studies over the years have examined the influences of vehicle design and flight environment parameter. Difficulties in obtaining accurate experimental results without corruption due to the test facility persist to this day. Given the difficulties in testing and the highly non-linear, coupled, and sensitive nature of the oscillatory behavior, the results of these studies have often been inconclusive and contradictory. The uncertainties associated with the expected damping characteristics force flight projects to carry large margins to minimize risk. In the last decade, a renewed effort to understand the governing principles and mechanisms that are responsible for the dynamic behavior of entry vehicles has provided further insight into the problem. Experimental verification of the proposed theories is still required and a dedicated effort to understand the governing mechanisms of dynamic stability would improve the understanding of blunt body and wake flow dynamics. Additionally, there is potential in utilizing the Mars Science Laboratory flight data to shed light onto this problem.

An improved understanding of dynamic stability fundamentals is critical as inflatable and deployable configurations begin to emerge. These more exotic entry configurations will introduce additional complexities into the system, such as the effect of a flexible aftbody. Given the deficiencies in the existing testing capabilities and the difficulties in scaling flexible materials, it will be challenging to simulate the dynamics of an inflatable decelerator at relevant sub-scale conditions. A focus on that the physics governing dynamic stability is required. With this improved understanding, vehicle and trajectory designs that improve the exploration capabilities of future planetary entry vehicles will result.

VIII. Acknowledgements

This work was supported by a NASA Office of the Chief Technologist's Space Technology Research Fellowship under NASA Grant #NNX11AN20H .

IX. References

[1] J. H. Allen, "Motion of a Ballistic Missile Angularly Misaligned With The Flight Path Upon Entering The Atmosphere and Its Effect Upon Aerodynamic Heating, Aerodynamic Loads, And Miss Distance," *NACA TN-4048*, 1957.

[2] M. Tobak and J. H. Allen, "Dynamic Stability of Vehicles Traversing Ascending or Descending Paths Through The Atmosphere," *NACA TN-4275*, 1958

[3] J. D. Bird, "Stability of Ballistic Reentry Bodies," *NACA RM L-58*, 1958.

[4] H. S. Fletcher, "Damping in Pitch and Static Stability of a Group of Blunt Bodies from M=0.6 to 0.95," *NASA TM X-194*, 1959.

[5] H. S. Fletcher and W. D. Wolhart, "Damping In Pitch and Static Stability of Supersonic Impact Nose Cones, Short Blunt Subsonic Impact Nose Cones, and Manned Reentry Capsules at Mach Numbers From 1.93 to 3.05," *NASA TM X-347*, no. November, Nov. 1960.

[6] B. J. Short and S. C. Sommer, "Some measurements of the dynamic and static stability of two blunt-nosed, low-fineness- ratio bodies of revolution in free flight at M=4," *NASA TM X-20*, 1959.

[7] D. A. Buell and N. S. Johnson, "An Experimental and Analytical Investigation of the Dynamics of Two Blunt Bodies at Subsonic Speeds," *NASA TM X-18*, 1959.

[8] B. H. Beam and E. C. Hedstrom, "Damping in Pitch of Bluff Bodies of Revolution at Mach Numbers from 2.5 to 3.5," *NASA TM X-90*, no. October, Nov. 1959.

[9] W. R. Wehrend Jr. and D. E. Reese Jr., "Wind-tunnel tests of the static and dynamic stability characteristics of four ballistic reentry bodies," *NASA TM X-369*, no. 1960, 1960.

[10] P. J. Tunnell, "The Static and Dynamic Stability Derivatives of a Blunt Half-Cone Entry Configuration at Mach Numbers from 0.7 to 3.5," *NASA TM X-577*, 1961.

[11] W. B. Igoe and E. R. Hillje, "Transonic dynamic stability characteristics of several models of Project Mercury capsule configurations," *NASA TM X-554*, 1961.

[12] W. R. Wehrend Jr., "An Experimental Evaluation of Aerodynamic Damping Moments of Cones With Different Centers of Rotation," *NASA TN D-1768*, no. March, 1963.

[13] M. Baillion, "Blunt Bodies Dynamic Derivatives," *AGARD-R-808 – Capsule Aerothermodynamics*, 1995.

[14] B. Dayman Jr., J. M. Brayshaw Jr., D. A. Nelson, P. Jaffe, and T. L. Babineaux, "The Influence of Shape on Aerodynamic Damping of Oscillatory Motion During Mars Atmosphere Entry and Measurement of Pitch Damping at Large Oscillation Amplitudes," *JPL TR 32-380*, 1963.

[15] M. Schoenenberger and E. M. Queen, "Limit Cycle Analysis Applied to the Oscillations of Decelerating Blunt-Body Entry Vehicles," *RTO-MP-AVT-152*, 2008.

[16] B. R. Wright and R. A. Kilgore, "Aerodynamic Damping and Oscillatory Stability in Pitch and Yaw of Gemini from 0.5 to 4.63," *NASA TN D-3334*, 1966.

[17] M. Tobak and V. L. Peterson, "Theory of Tumbling Bodies Entering Planetary Atmospheres with Application to Probe Vehicles" *NASA TR R-203*, 1964.

[18] I. M. Jaremenko, "Wakes Their Structure and Influence Upon Aerodynamic Decelerators," *NASA CR-74*, 1967.

[19] S. Teramoto, K. Fujii, and K. Hiraki, "Numerical Analysis of Dynamic Stability of a Reentry Capsule at Transonic Speeds," *AIAA 98-4451, AIAA Journal 39-4*, vol. 39, no. 4, pp. 646-653, Apr. 2001.

[20] D. B. Owens and V. V. Aubuchon, "Overview of Orion Crew Module and Launch Abort Vehicle Dynamic Stability," *AIAA 2011-3504*, 2011.

[21] C. H. Whitlock and P. M. Siemers, "Parameters Influencing Dynamic Stability Characteristics of Viking-Type Entry Configurations at Mach 1.76," *Journal of Spacecraft and Rockets*, vol. 9, no. 7, pp. 558-560, Jul. 1972.

[22] W. C. ; Moseley Jr., R. H. J. ; Moore, and J. E. Hughes, "Stability Characteristics of the Apollo Command Module," *NASA TN D-3890*, 1967.

[23] G. T. Chapman and L. A. Yates, "Dynamics of Planetary Probes : Design and Testing Issues," *AIAA 1998-0797*, 1998.

[24] J. P. Reding and L. E. Ericsson, "Dynamic Support Interference," *Journal of Spacecraft and Rocket*, vol. 9, no. 7, pp. 547-553, Jul. 1972.

[25] B. L. Uselton and F. B. Cyran, "Sting Interference Effects as Dynamic Stability Derivatives, Surface Pressure, and Base Pressure for Mach Numbers 2 through 8," *AEDC TR 79-89*, 1980.

[26] S. Steinberg, B. L. Uselton, and P. M. Siemers, "Viking configuration pitch damping derivatives as influenced by support interference and test technique at transonic and supersonic speeds," *AIAA-1972-1012*, 1972.

[27] B. Dayman Jr., "Optical Studies of Free-Flight Wakes," *JPL TR No. 32-364*, Nov. 1962.

[28] L. E. Ericsson and J. P. Reding, "Aerodynamic Effects of Bulbous Bases," *NASA CR-1339*, Aug. 1969.

[29] L. E. Ericsson and J. P. Reding, "Re-Entry Capsule Dynamics," *Journal of Spacecraft and Rockets*, vol. 8, no. 6, 1971.
[30] R. A. East and G. R. Hutt, "Comparison of predictions and experimental data for hypersonic pitching motion stability," *Journal of Spacecraft and Rockets*, vol. 25, no. 3, pp. 225-233, May. 1988.
[31] A. Seiff, "Secondary Flow-Fields Embedded in Hypersonic Shock Layers," *NASA TN D-1304*, May 1962.
[32] A. Seiff, and E. E. Whiting, "Calculation of Flow Fields from Bow-Wave Profiles for the Downstream Region of Blunt-Nosed Circular Cylinders in Axial Hypersonic Flight," *NASA TN D-1147*, Nov. 1961
[33] A. Seiff and E. E. Whiting, "Correlation of the Bow-Wave Profiles of Blunt Bodies," *NASA TN-D 1148*, Feb. 1962.
[34] L. E. Ericsson, "Unsteady Embedded Newtonian Flow," *Astronautical Acta*, Vol 18, Nov. 1973, pp. 309-330.
[35] L. E. Ericsson, "Generalized Unsteady Embedded Newtonian Flow," *Journal of Spacecraft and Rockets*, vol. 12, no. 12, pp. 718-726, Dec. 1975.
[36] B. G. Tong and W. H. Hui, "Unsteady Embedded Newton-Busemann Flow Theory," *Journal of Spacecraft and Rockets*, vol. 23, no. 2, pp. 129-135, Mar. 1986.
[37] S. M. Murman, "Reduced-Frequency Approach for Calculating Dynamic Derivatives," *AIAA Journal*, vol. 45, no. 6, pp. 1161-1168, Jun. 2007.
[38] S. M. Murman and M. J. Aftosmis, "Dynamic Analysis of Atmospheric-Entry Probes and Capsules," *AIAA 2007-74*, no. January, pp. 1-18, 2007.
[39] S. M. Murman, "Dynamic Viscous Simulations of Atmospheric-Entry Capsules," *AIAA 2008-6911*, 2008.
[40] E.Stern, V. Gidzak, and G. Chandler, "Estimation of Dynamic Stability Coefficients for Aerodynamic Decelerators Using CFD," *AIAA Applied Aerodynamics Conference*, New Orleans, LA, June 2012, *AIAA-2012-3225*
[41] B. L. Uselton, T. O. Shadow, and A. C. Mansfield, "Damping in Pitch Derivatives of 120 and 140 Degree Blunted Cones at Mach Numbers of 0.3 through 3," *AEDC TR 70-49*, 1972.
[42] G. T. Chapman, W. H. Hathaway, and R. A. Mitcheltree, "Transonic and Low Supersonic Static and Dynamic Aerodynamic Characteristics of the Stardust Sample Return Capsule," *AIAA 1999-1021*, 1999.
[43] R. H. Prislin and P. Jaffe, "Angle-of-Attack Motion of a Spinning Entry Vehicle," *Journal of Spacecraft and Rockets*, vol. 6, no. 1, Jan. 1969
[44] P. Jaffe, "Dynamic Stability Tests of Spinning Entry Bodies in the Terminal Regime," *Journal of Spacecraft and Rockets*, vol. 8, no. 6, pp. 575-579, Jun. 1971.
[45] W. J. Marko, "Dynamic Stability of High-Drag Planetary Entry Vehicles at Transonic Speeds," *Journal of Spacecraft and Rockets*, vol. 6, no. 12, pp. 1390-1396, Dec. 1969
[46] E. Slimko, G. L. Winchenbach, and Y. M. Lipnitsky, "Transonic Dynamic Stability Instigations of a 45 degree Sphere-Cone with a Hemispherical Afterbody (Mars Microprobe)," *15th AIAA Applied Aerodynamics Conference*, 1996.
[47] J.H. Allen and A. J. Eggers Jr., "A Study of the Motion and Aerodynamic Heating of Missiles Entering the Earth's Atmosphere at High Supersonic Speeds," *NACA TN 4047*, 1957
[48] M. V. Krumins, "Drag and Stability of Mars Probe/Lander Shapes," *Journal of Spacecraft and Rockets*, vol. 4, no. 8, pp. 1052-1057, Aug. 1967.
[49] L. E. Ericsson, "Effect of boundary-layer transition on vehicle dynamics," *Journal of Spacecraft and Rockets*, vol. 6, no. 12, pp. 1404-1409, Dec. 1969.
[50] R. I. Sammonds, "Transonic Static and Dynamic Stability Characteristics of Two Large Angle Spherically Blunted High Drag Cones," *AIAA 70-564*, 1970.
[51] R.A. Mitcheltree, J. N. Moss, F. M. Cheatwood, F.A. Greene, and R.D. Braun, "Aerodynamics of the Mars Microprobe Entry Vehicles," *AIAA-97-3658*, 1997
[52] H. G. Wiley, R. A. Kilgore, and E. R. Hillje, "Dynamic Directional Stability for a Group of Blunt Reentry Bodies at Transonic Speeds," *NASA TM X -337*, 1960.
[53] G. T. Chapman, C. Berner, W. H. Hathaway, and G. L. Winchenbach, "The Use of Spherical Bases to Eliminate Limit Cycles of Blunt Entry Vehicles," *AIAA-1999-1023*, 1999.
[54] M. Schoenenberger, L.A. Yates, and W. H. Hathaway, "Dynamic Stability Testing of the Mars Science Laboratory Entry Capsule," *AIAA 2009-3917*, 2009.
[55] B. Smith, "Oscillation of Supersonic Inflatable Aerodynamic Decelerators at Mars," Masters Project, Georgia Institute of Technology, 2010.
[56] I. G. Clark, "Aerodynamic Design, Analysis, and Validation of a Supersonic Inflatable Decelerator," Ph.D. Thesis, Georgia Institute of Technology, 2009.

[57] A. L. Ramsey and G. T. Chapman, "A Study of Reynolds Number Effects on Supersonic Flow Over Blunt Bodies," *AIAA 2000-1010*, 2000.
[58] E. R. Hillje and A. O. Pearson, "Transonic Static and Dynamic Longitudinal Stability Characteristics of a Low-Fineness-Ratio, Blunted-Cylinder Reentry Body Having a Converging-Cone Afterbody," *NASA TM X -672*, 1966.
[59] F. Y. Wang, O. Karatekin, and J. M. Charbonnier, "An Experimental Study of the Flow-Field Around an Apollo Capsule at Low Speed," *AIAA-98-0319*, 1997.
[60] F. Y. Wang, J. M. Charbonnier, O. Karatekin, and S. Paris, "The Utilization of Low Speed Facilities in Transonic Stability of Reentry Vehicles Research - An Evaluation," *AIAA 98-2636*, 1998.
[61] F. Y. Wang, J. M. Charbonnier, and O. Karatekin, "Low-Speed Aerodynamics of a Planetary Entry Capsule," *Journal of Spacecraft and Rockets*, vol. 36, no. 5, pp. 659-667, Sep. 1999.
[62] J. R. Micol, "Simulation of Real-Gas Effects on Pressure Distribution for a Proposed Aeroassit Flight Experiment Vehicle," *AIAA-87-2368, 1987.*
[63] R.A. Jones and J. L. Hunt "Measured Pressure Distributions on Large Angle Cones in Hypersonic Flows of Tetrafluoromethane, air and Helium" *NASA TN D-7429*, 1974.
[64] L. E. Ericsson and J. P. Reding, "Ablation Effects on Vehicle Dynamics," *Journal of Spacecraft and Rockets*, vol. 3, no. 10, pp. 1476-1483, Oct. 1966.
[65] L. E. Ericsson, "Unsteady Aerodynamics of an Ablating Flared Body of Revolution Including Effect of Entropy Gradient," *AIAA Journal*, vol. 6, no. 12, pp. 2395-2596, Dec. 1968.
[66] J. H. Grimes Jr., and J. J. Casey, "Influence of Ablation on the Dynamics of Slender Re-Entry Configurations," *Journal of Spacecraft and Rockets*, vol. 2, no. 1, pp. 106-108, 1965.
[67] T. Abe, S. Sato, Y. Matsukawa, K. Yamamoto, and K. Hiraoka, "Study for Dynamically Unstable Motion of Reentry Capsule," *AIAA-2000-2589*, 2000.
[68] K. Hiraki, Y. Inatani, N. Ishii, T. Nakajima, and M. Hinada, "Dynamic Stability of Muses-C Capsule," *21st International Symposium on Space Technology, ISTS 98-d-33*, 1998.